



IEA Wind Energy Task 37 System Engineering Aerodynamic Optimization Case Study

Preprint

Michael K. McWilliam,¹ Katherine Dykes,¹ Frederik Zahle,¹
Pietro Bortolotti,² Andrew Ning,³ Evan Gaertner,⁴
Terence Macquart,⁵ Karl Merz,⁶ Ainara Irisarri Ruiz⁷

1 Technical University of Denmark

2 National Renewable Energy Laboratory

3 Brigham Young University

4 University of Massachusetts Amherst

5 University of Bristol

6 SINTEF

7 National Renewable Energy Center

*Presented at the 2021 AIAA SciTech Forum
January 11–21, 2021*

**NREL is a national laboratory of the U.S. Department of Energy
Office of Energy Efficiency & Renewable Energy
Operated by the Alliance for Sustainable Energy, LLC**

This report is available at no cost from the National Renewable Energy Laboratory (NREL) at www.nrel.gov/publications.

Contract No. DE-AC36-08GO28308

Conference Paper
NREL/CP-5000-78593
March 2021



IEA Wind Energy Task 37 System Engineering Aerodynamic Optimization Case Study

Preprint

Michael K. McWilliam,¹ Katherine Dykes,¹ Frederik Zahle,¹ Pietro Bortolotti,² Andrew Ning,³ Evan Gaertner,⁴ Terence Macquart,⁵ Karl Merz,⁶ Ainara Irisarri Ruiz⁷

1 Technical University of Denmark

2 National Renewable Energy Laboratory

3 Brigham Young University

4 University of Massachusetts Amherst

5 University of Bristol

6 SINTEF

7 National Renewable Energy Center

Suggested Citation

McWilliam, Michael K., Katherine Dykes, Frederik Zahle, Pietro Bortolotti, Andrew Ning, Evan Gaertner, Terence Macquart, Karl Merz, Ainara Irisarri Ruiz. 2021. *IEA Wind Energy Task 37 System Engineering Aerodynamic Optimization Case Study: Preprint*. Golden, CO: National Renewable Energy Laboratory. NREL/CP-5000-78593. <https://www.nrel.gov/docs/fy21osti/78593.pdf>.

**NREL is a national laboratory of the U.S. Department of Energy
Office of Energy Efficiency & Renewable Energy
Operated by the Alliance for Sustainable Energy, LLC**

This report is available at no cost from the National Renewable Energy Laboratory (NREL) at www.nrel.gov/publications.

Contract No. DE-AC36-08GO28308

Conference Paper
NREL/CP-5000-78593
March 2021

National Renewable Energy Laboratory
15013 Denver West Parkway
Golden, CO 80401
303-275-3000 • www.nrel.gov

NOTICE

This work was authored in part by the National Renewable Energy Laboratory, operated by Alliance for Sustainable Energy, LLC, for the U.S. Department of Energy (DOE) under Contract No. DE-AC36-08GO28308. Funding provided by the U.S. Department of Energy Office of Energy Efficiency and Renewable Energy Wind Energy Technologies Office. The views expressed herein do not necessarily represent the views of the DOE or the U.S. Government. The U.S. Government retains and the publisher, by accepting the article for publication, acknowledges that the U.S. Government retains a nonexclusive, paid-up, irrevocable, worldwide license to publish or reproduce the published form of this work, or allow others to do so, for U.S. Government purposes.

This report is available at no cost from the National Renewable Energy Laboratory (NREL) at www.nrel.gov/publications.

U.S. Department of Energy (DOE) reports produced after 1991 and a growing number of pre-1991 documents are available free via www.OSTI.gov.

Cover Photos by Dennis Schroeder: (clockwise, left to right) NREL 51934, NREL 45897, NREL 42160, NREL 45891, NREL 48097, NREL 46526.

NREL prints on paper that contains recycled content.

IEA Wind Energy Task 37 System Engineering Aerodynamic Optimization Case Study

Michael K. McWilliam*, Katherine Dykes and Frederik Zahle

Wind Energy Department, Technical University of Denmark, Frederiksborgvej 399, 4000 Roskilde, Denmark

Pietro Bortolotti

National Wind Technology Center, National Renewable Energy Laboratory, 18200 CO-128, Boulder, CO 80303, USA

Andrew Ning

Brigham Young University, Provo, UT 84602, USA

Evan Gaertner

University of Massachusetts Amherst, Amherst, MA 01003, USA

Terence Macquart

University of Bristol, Senate House, Tyndall Ave, Bristol BS8 1TH, United Kingdom

Karl Merz

SINTEF, P.O. Box 4760 Torgarden, NO-7465 Trondheim, Norway

Ainara Irisarri Ruiz

National Renewable Energy Center, CENER, Av. Ciudad de la Innovacion, 7, 31621, Sarriguren, Navarra, Spain

This paper presents the results from the first IEA Wind Task 37 aerodynamic optimization case study. Eight participants applied their optimization tools to a purely aerodynamic problem and the results were compared. Overall, the different tools produced widely different designs, while there was better agreement in the improvement achieved. This highlights the fact that further investigation is needed to try to understand these differences and develop best practices. There were too many differences between the different analysis and optimization codes to determine the sources of these differences. However, several potential sources of discrepancy were identified for further investigation. One hypothesis is that one potential source of discrepancy is that the design problem itself is relatively flat in design directions of constant loading. This flatness would impact the convergence in the optimization, and at the same time mean that discrepancies in the design itself would be less severe.

I. Introduction

Numerical optimization is a powerful tool for design. Within the literature, there are many examples of highly advanced multi-disciplinary design optimization frameworks performing aero-servo-elastic design simultaneously [1–10]. Many of the different authors apply different techniques and optimization framework structures to achieve these results. One of the objectives of the IEA Wind Task 37 on system engineering is to conduct focused studies on numerical design optimization to obtain a better understanding of these methods and to develop a set of best practices. To make these investigations tractable, the first test case is a purely aerodynamic optimization test case that is described here along with the results. Eight institutes participated and applied their tools in this investigation. This paper shows the results of this comparison and includes a discussion.

This paper is organized into four sections. First, the description of the test case is given in Section II. For the purpose of reproduction, all the details of this test case are given in the appendix. Each participant was asked to report on the details of their analysis and optimization tools, along with amount of human and computational effort expended. These results are given in Section III. To quantify the differences in the analysis tools, each participant was asked to show the predicted performance of the initial design. These results are shown in Section IV. Finally, the participants were asked

*mimc@dtu.dk

to optimize the turbine and share both the optimal designs and the predicted performance of that design. These results are shown in Section V. Finally, Section VI gives a discussion on these results, followed by conclusions in Section VII.

The exact source of all the results is kept anonymous for several reasons. First, the authors want to avoid a comparison between the institutes themselves. Furthermore, the comparison is not completely fair. Some bias could have been introduced as the test case was developed by the tool chain of Participant 1. While the different participants have frameworks at different levels of maturity, developed for different purposes, thus some may be more or less suited for this particular test case. The focus of this study is on how all these differences in the analysis and optimization lead to different outcomes in the solutions.

II. Test Case Description

The initial design for the test case is based loosely on the DTU 10-MW Reference Wind Turbine design [11]. Since this design was already optimized aerodynamically, there was some concern that this initial design would not give enough design freedom to allow for a meaningful comparison. To avoid this, the chord and twist distributions were scaled to reduce the overall loading and give a sub-optimal design. The modified chord and twist distributions are given in Figure 1 along with the data from the original DTU 10-MW Reference Wind Turbine design. The initial design was further modified to remove tilt, coning and pre-bend so that unsteady and 3D aerodynamic effects would not be relevant in the analysis.

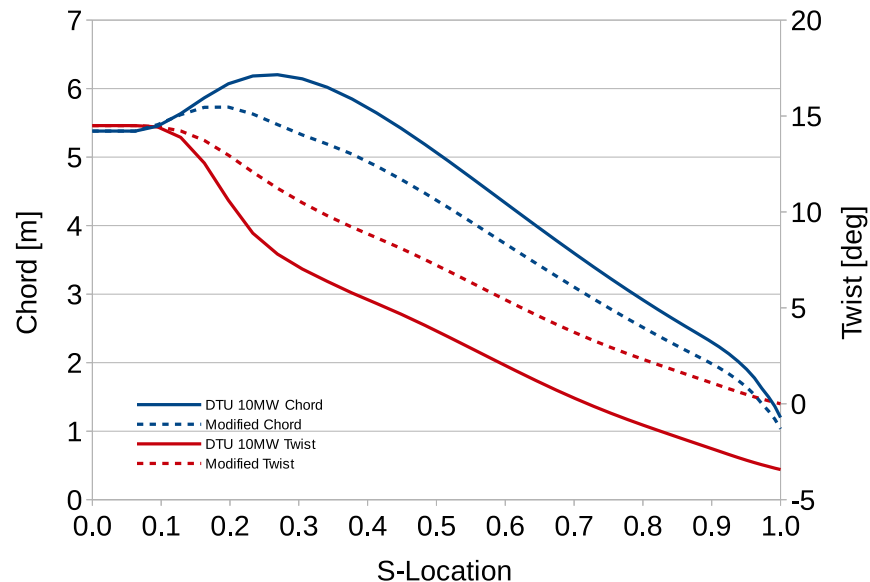


Fig. 1 The chord and twist of the initial design compared with the DTU 10-MW Reference Wind Turbine

Along with the plan-form properties, the test case also provided the airfoil data for a cylindrical profile, FFA-W3-600, FFA-W3-480, FFA-W3-360, FFA-W3-301 and FFA-W3-241 profile. The test case provided 2D airfoil shapes, but these data were not used in any of the optimization results given here.

The objective was to maximize the Annual Energy Production (AEP) according to a given wind speed distribution loosely based on a Class I site. The wind was assumed to be steady and uniform with no shear, turbulence or yaw error. The air density was specified to be 1.225 kg/m^3 .

Structural aspects were incorporated into the optimization problem by specifying a minimum absolute thickness constraint shown in Figure 2. Furthermore, a rotor thrust and root flap-wise bending moment constraint was included to limit the loads. To avoid tool differences affecting these constraints, these load constraints were specified relative to the corresponding load of the initial design. The constraint limit allowed for a 14% increase in the thrust along with a 11% increase in the root flap-wise bending moment. A combination of these two constraints would prevent the optimization from moving towards maximum C_P designs.

To remove the effects of different controllers, the regulation of the turbine was specified. The maximum mechanical power was 10.6383 MW. The minimum and maximum rotational speed was 6.0 and 9.6 RPM respectively. The turbine

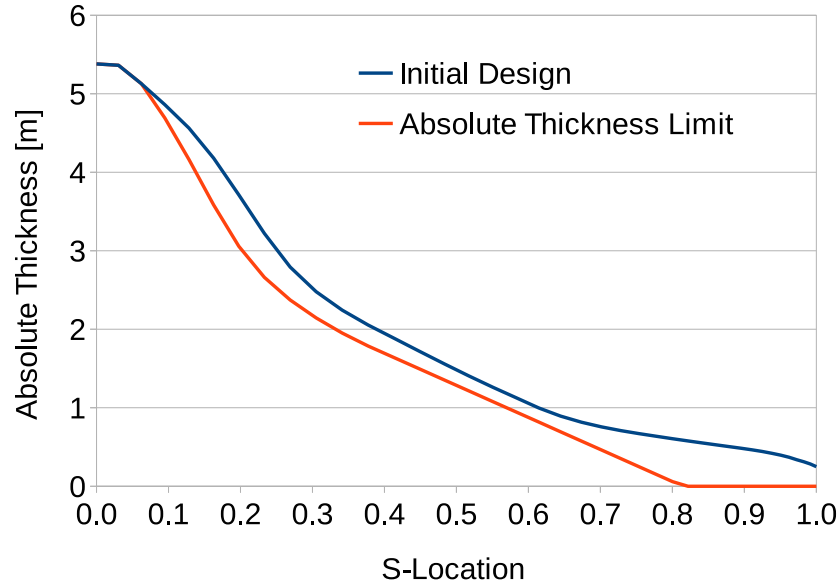


Fig. 2 Minimum absolute thickness constraint

is meant to operate as a standard pitch to feather regulated, variable speed machine. Within the variable speed region, the rotor should operate at a tip speed ratio of 7.8. Above rated conditions, the rotor should pitch to feather to avoid exceeding the maximum power constraint. For these high wind speeds, the participants were responsible for determining the required pitch according to their tools. The participants were free to use pitch to optimize performance when the rotor reached the minimum speed, but not in the variable speed region.

The design variable for this problem was the chord and twist distribution for the blade. Additionally, the participants could vary the airfoil distribution along the blade. The plan-form variables at the root of the blade are fixed in the optimization. Furthermore, the length of the blade nor any of the regulation parameters could be changed.

In summary, the optimization problem is given in Equation (1).

$$\begin{aligned}
 & \text{Maximize} && \text{Annual energy production} \\
 & \text{Varying} && \\
 & && \text{Chord} \\
 & && \text{Twist} \\
 & && \text{Relative thickness} \\
 & \text{subject to} && \\
 & && T \leq 1.14 \max T_0, \\
 & && M \leq 1.11 \max M_0, \\
 & && \text{Absolute thickness} \geq \text{limit} \\
 & && \text{Basic regulation constraints}
 \end{aligned} \tag{1}$$

For the purpose of reproduction, all the data for the test case is given in the Appendix A in tabular form.

It should be noted that the tool chain of Participant 1 was used to develop this test case. In developing the test case, multiple problems were solved with varying constraint limits. The test case here was chosen partly because it showed stable performance with this tool chain. Thus, there might be an unintentional bias in the results due to this.

III. Participant Survey

To understand the tools behind the results, the participants were asked to fill out a survey on the analysis and optimization. Not all participants provided completed surveys furthermore, Participant 8 provided survey results and

no optimization results. However, to map these survey results to the optimization and analysis results, the participant numbering is kept consistent throughout the text. The participants were asked about whether they used various submodels (*e.g.* tip-loss, turbulent wake, *etc.*) within the analysis and to specify the versions of these submodels. Some users specified that they used a submodel but did not give any details; in these cases, the tables simply list “Yes”.

Table 1 summarizes the results on the aerodynamic analysis. Overall, the participants were using standard Blade Element Momentum (BEM) models. Some users are using an unsteady BEM model typically these are corrected steady models, where the effect of the correction decays to zero in steady conditions. Another major difference is the use of a hub-loss model, which should affect the analysis towards the root portion of the blade. Some participants employ a yaw correction, but this should not be relevant in this test case.

Table 1 Summary of the Aerodynamic Analysis Models

Participant	Aerodynamic Model	Angular Momentum	Tip Loss	Turbulent Wake	Other Sub-models
1	Steady BEM	Yes	Prandtl	Yes	Yaw
2	Unsteady BEM	N/A	N/A	No	N/A
3	Steady BEM	Yes	Prandtl	Burton	No
4	Unsteady BEM	Yes	Prandtl	Yes	Hub loss
5	Unsteady BEM	Yes	Prandtl	No	Hub loss
6	Steady BEM	Yes	Prandtl	Buhl	Yaw and reversed flow
8	Steady BEM	N/A	N/A	Yes	Hub loss

The participants were asked about special features that may or may not be relevant to this test case. Participants 2, 3, 4 and 5 all reported using both a dynamic wake and a dynamic stall models in the analysis. The effect of these models should decay away in steady conditions. The analysis of participant 5 is based on the aero-structural model of FAST 8. The test case specifies that the blades should be rigid; thus, it is assumed that elastic deformation was not modeled. The model of Participant 3 is capable of solving the equations in the frequency domain; however this analysis is not relevant for this test case.

Table 2 summarizes the parameterization of the design variables and the optimization algorithms used by the participants. All the participants used splines in the parameterization; typically approximately 15 design variables were used in total, with one participant using 36 design variables. A wide variety of optimization algorithms and stopping criteria were used in the case study. All the optimization algorithms were gradient based, with the exception of participant 5 who used a genetic algorithm. Furthermore, a wide range of stopping conditions were employed. The wide variance in the optimization algorithms could be a source of differences in the optimal solutions.

Table 2 Summary of the Parameterization and Optimization Algorithms

Participant	Parameterization	Number of Design Variables	Optimization Algorithm	Stopping Criteria
1	Bezier free form deformation splines	13	IPOPT [12]	10^{-6} tolerance
2	1 st order splines	39	MATLAB fmincon	10^{-8} tolerance
3	Splines	18	Octave SQP	No decreasing direction
4	Splines	15	SQP	Iterative convergence
5	Splines	15	Genetic (NSGA-II [13])	Number of generations
6	Splines	15	SQP	10^{-6} tolerance
8	Akima	14	Sequential least squares	200 Iterations Max

The participants were asked to give additional details on the optimization. Participant 5 reported the following settings for the optimization: probability of mating two individuals $CXPB = 0.9$; crowding degree of mutation $\eta_{mutate} = 20$; and crowding degree of cross over, $\eta_{mate} = 20$. Participant 3 reported the use of penalty functions for the constraints. Participant 3 also reported that within the optimization only performed analysis below rated conditions. Participant 3 also normalized both the objective and the constraint values so that they would be close to unity.

Table 3 summarizes the coupling code and the gradient algorithms that were used in their framework. The coupling code describes how the analysis was coupled to the optimization. Most users used pure Python or MATLAB, while two participants use the dedicated package OpenMDAO. A majority of the participants used some form of finite differencing for the gradient calculations. However, Participant 6 used analytic gradients via Tapenade, which should improve the convergence in the optimization. Additionally, Participant 3 used complex step gradient algorithms, which should also improve the accuracy of the gradients and subsequently the convergence in the optimization as well. However, complex step methods may still have errors relative to analytic gradients. Participant 2 reported that they performed an extensive study to tune the gradient step-size.

Table 3 Summary of the Coupling and Gradient Calculation

Participant	Coupling Code	Gradient Algorithm	Gradient Step Size
1	OpenMDAO	First order forward Euler	10^{-2}
2	MATLAB	Finite difference	10^{-6}
3	N/A	Complex step with some finite difference	10^{-4}
4	N/A	Central differencing	4% of bounds
5	OpenMDAO	N/A	N/A
6	Python	Reverse automatic differentiation with Tapenade	N/A
8	MATLAB and Python	Central differencing	10^{-2}

The participants were asked to describe additional special features of their optimization framework. Participant 5 reported that their tool is primarily used for offshore wind turbines.

The participants were asked to report on both the human effort and the computational effort that was required to obtain the results. Participant 2 described their human effort as follows: “A couple of days tuning the optimization. Unspecified amount of time on making the code sufficiently robust. 2 hours wrapping the simulation code for the optimization. A couple hours creating some post-processing functionality. 4-5 hours validating the optimization, more time could be needed. 3-4 hours setting up the input files. 1-2 hours fixing problems. 2 hours tuning the gradients. 1 day performing exploration studies. Minutes Setting up a single optimization.” Participant 3 described their human effort as follows: “2 hours verifying complex step. 1 hour trying to speed up the code. 4 hours implementing a getAEP function. 2 hours writing post-processing functions. 4 hours validating the optimization. 2 hours creating a custom input for this problem.”

Participant 2 described the computational effort for the problem as follows. They report both the calculation time for fmincon and a GA because they tried both in their preliminary studies, but they submitted the final results from fmincon. “With a I7-4790 CPU at 3.6 GHz with 16 GB RAM it took 10 hours calculation for all the studies, 1-2 hours for fmincon, 5 hours for GA.” Participant 3 described the computational effort as follows: “With a serial CPU 200 hours of calculation for everything and 12 hours for a single calculation.”

Overall, the survey results show that most of the users used a standard BEM model with the standard correction models. Thus, it is unlikely that the analysis should provide significant differences in the results. The biggest differences between the frameworks used by all the participants is in the set-up of the optimization. Most users employed a gradient-based algorithm with spline parameterization and finite difference gradients. A notable difference is Participant 5 who used genetic algorithms and Participant 6 who used analytic gradients.

IV. Initial Design Performance

The first study in the comparison was of the performance of the initial design. There are two main sources of differences in comparing optimization results: the differences in the analysis for the same design and the difference in the optimal design. So, differences in the optimization results can be a result of both types of error. So The purpose of this study was to assess the level of agreement in the analysis and show the first main source of error.

Figure 3 shows the power predicted of the initial design by each of the participants. The figure shows that the differences in power can be seen, but they are small. Figures 4 and 5 show the predicted values of the load constraints. The predicted thrust shows slightly larger differences, but it is the predicted root flap-wise bending moment that shows the greatest differences in the tools. Figure 6 shows the predicted pitch needed to maintain constant power above rated conditions. The figure shows only small differences, but the predicted pitch would have no impact on the AEP and no impact on the loads. Overall, if the differences in the optimization results are due to the analysis, they are first likely differences in the predicted bending moment, followed by thrust.

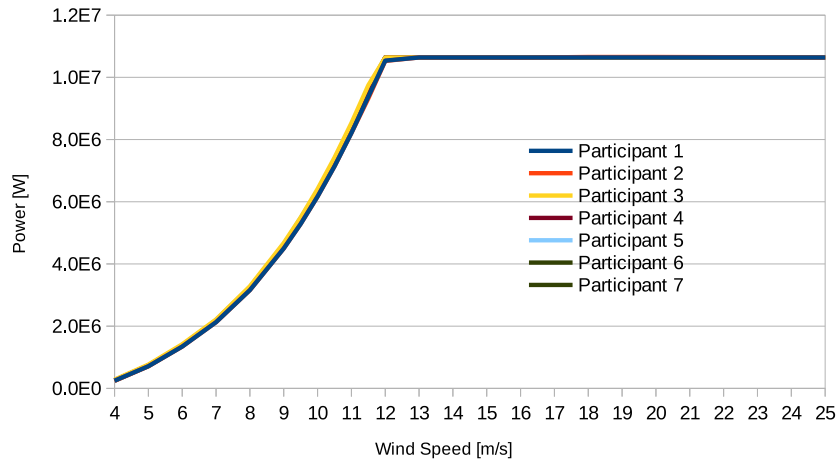


Fig. 3 The power of the initial power

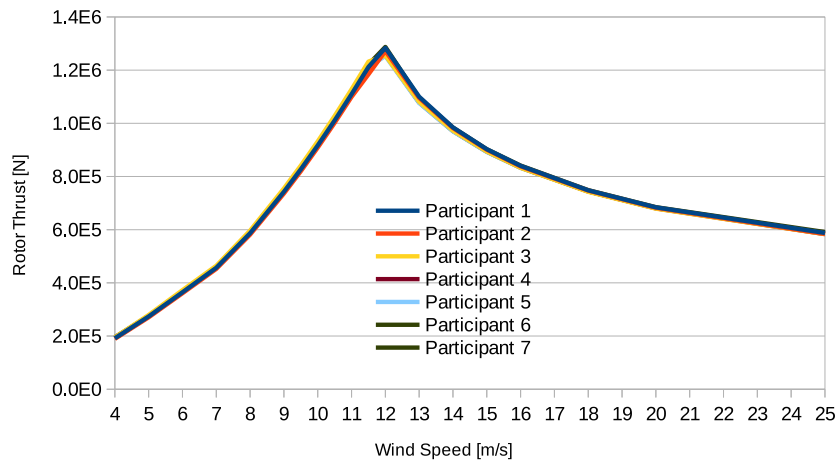


Fig. 4 The power of the initial root flap-wise moment

V. Blind Results Comparison

All the participants were given the design problem without seeing the results of another participant. This prevented a user from tuning the optimization to acquire results in better agreement. Thus, the results presented here show the full range of different solutions one could expect to obtain using the different optimization methods and analysis tools used in this study.

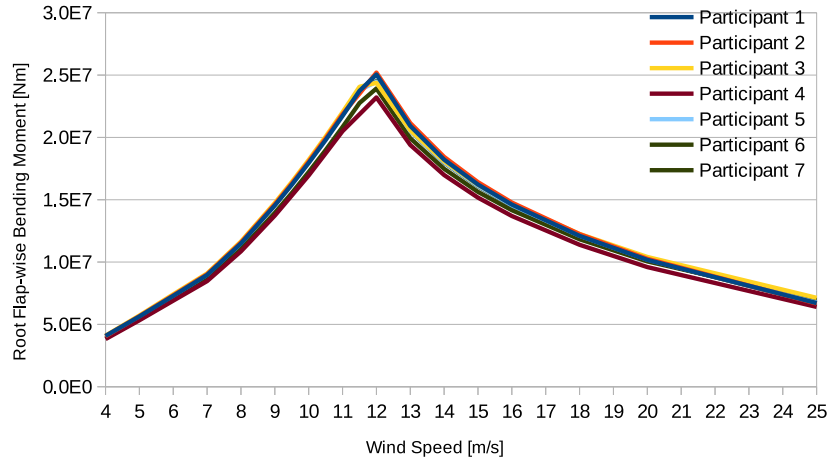


Fig. 5 The power of the initial root flap-wise moment

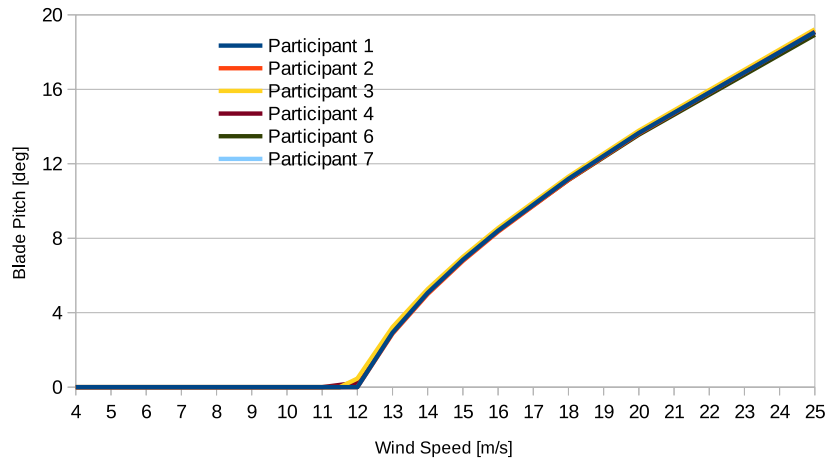


Fig. 6 The power of the initial root blade pitch

This section is divided into two sections. The first (Section V.A) shows the designs obtained from each of the different participants in the optimization. The second (Section V.B) gives the performance of the optimal designs as reported by the different participants.

Participant 3 provided a second set of results that did use pitch in the variable speed region for peak-shaving; because of the increased design freedom, these results are not directly comparable to the other results. For the sake of interest, these results will still be presented. They are differentiated by the tag “fix” or “free”, where the fixed results had fixed pitch in the variable speed region and free allowed for peak shaving; only the fixed results are consistent with the results of the other participants.

A. Optimal Design

Figures 7 through 9 show the optimal planform design, as predicted by the different participants. All the optimization results showed large increases in the chord, especially towards the root of the blade. These designs are not realistic, since they would exceed the maximum chord for industrial design. A maximum chord constraint was not included intentionally so that the design is purely a result of the optimization and not due to an a-priori constraint limit value. Furthermore, since this is a purely aerodynamic optimization, Figure 9 is showing that the different optimizations are driving towards thinner and more efficient airfoil sections.

Overall, the different designs do not show a strong agreement, with the largest differences occurring towards the root of the blade and again showing divergence towards the tip of the blade. Yet in the mid-span of the blades, the different results showed better agreement. It should be noted that Section V.B will show that participant 2 did not achieve full convergence, so differences between Participant 2 and the others may be attributed to a lack of convergence. Further discussion of these differences will be given in Section VI.

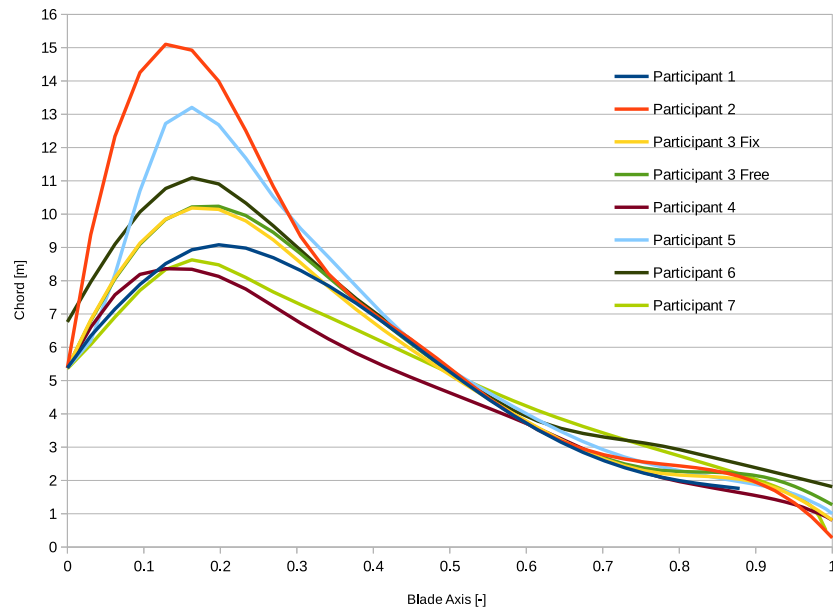


Fig. 7 The chord of the optimal design

Figure 10 shows the absolute thickness for each of the optimal designs. Most of the results respected the absolute thickness limit. However, Participant 2 showed some minor violations of this constraint for both the “fixed” and “free” results. This constraint is active in the mid-span for most participants. This could explain why better agreement in both chord and twist was achieved in this region, as one aspect of the design is specified by this limit.

Figure 11 shows the pitch schedule of all the different optimization results. Overall, all the participants pitched the blade to feather in the lower wind speeds to lower the thrust to avoid turbulent wake state. Then later all the participants used pitch to maintain constant power above rated. In these two regions, most of the results are within 2° of each other.

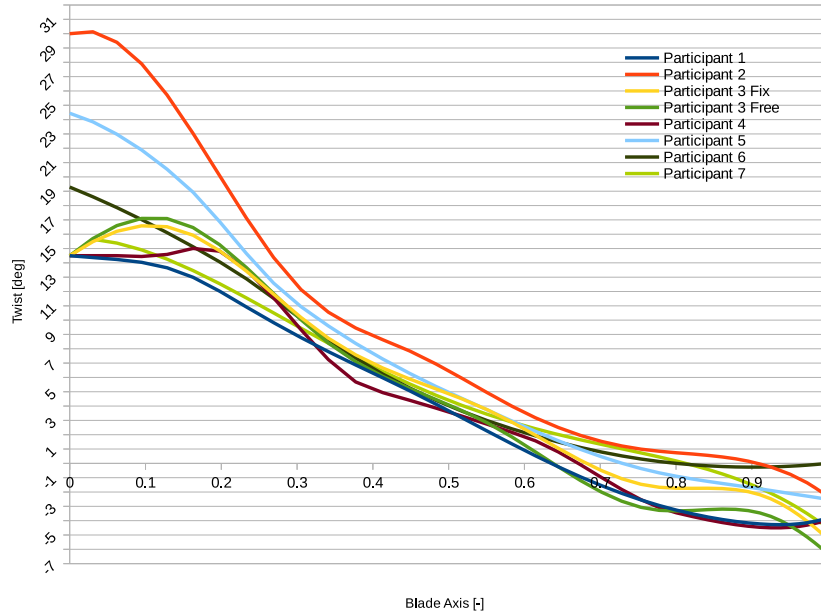


Fig. 8 The twist of the optimal design

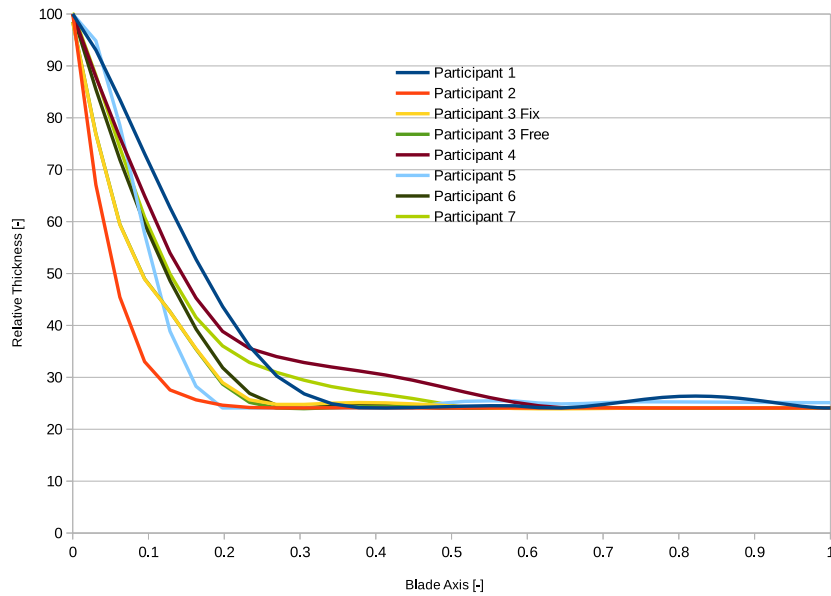


Fig. 9 The relative thickness of the optimal design

B. Optimal Performance

Table 4 shows all but one of the participants were able to achieve an improvement between 10 and 12.5% in the AEP. The table shows that neither load constraint is active for Participant 2, while their improvement in AEP is below that of the other participants. This shows that it is likely that their optimization was not able to achieve full convergence. For the remaining participants, the root flap-wise bending moment constraint is active, and Participant 5 is exceeding this constraint. The thrust constraint is only active for Participant 1.

Figure 12 shows the optimal power curve for all the participants. As expected, all the participants improved the power below rated conditions. Figure 13 shows the increase in AEP achieved at each of the different wind speeds, while

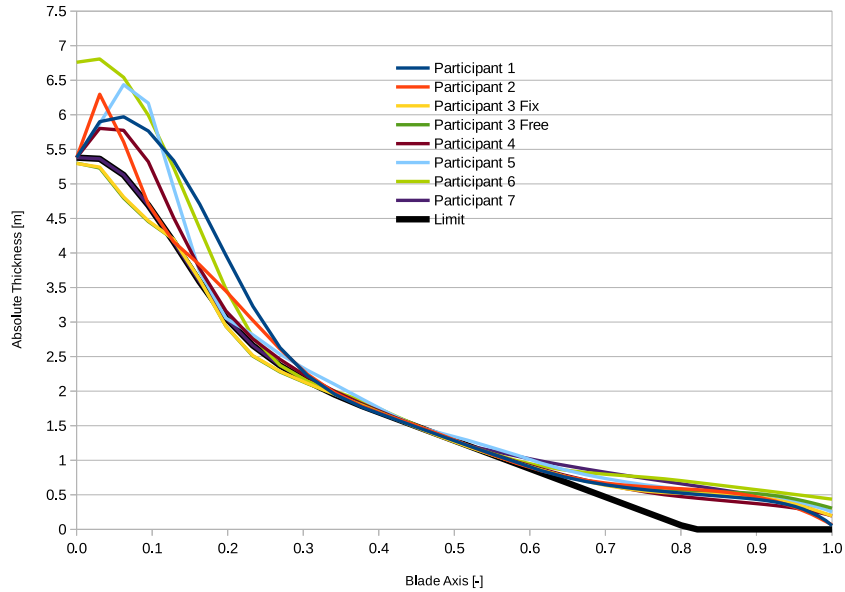


Fig. 10 The absolute thickness of the optimal design

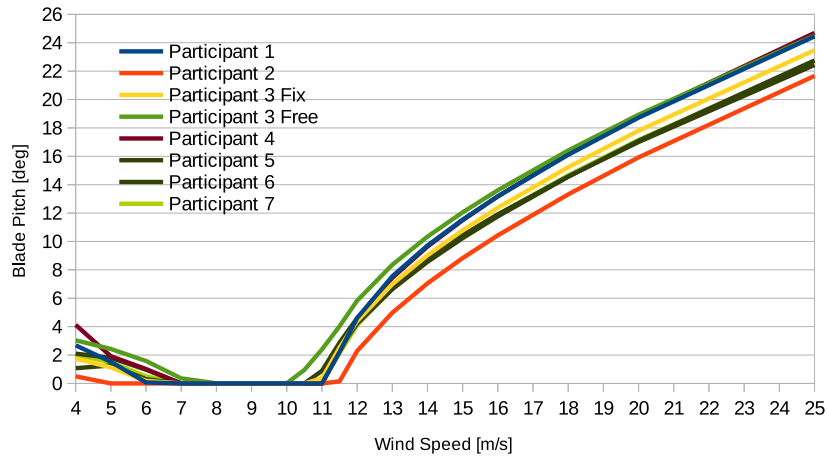


Fig. 11 The pitch of the optimal design

Figure 14 shows the ratio of power versus the power of the initial design. The results show that most of the improved production is occurring in the variable speed region. Furthermore, the different optimization frameworks are showing good agreement in power in this region. The greatest differences in power occur when the minimum rotor speed is reached and the optimization can use pitch to avoid turbulent wake state. Here the different frameworks achieved between no improvement and 36%.

Figure 15 shows the thrust curves of the optimal designs, while Figure 16 shows the root flap-wise bending moment of the optimal designs. As expected for all optimization results, the thrust and root flap-wise bending moment increased up until rated conditions and then decreased once the blades pitched to feather. Again, the free results from participants 3 are not comparable, while the Participant 2 optimization is likely not converged. Aside from these two results, the thrust shows good agreement between the participants. However, the bending moment results show the greatest disagreement between all the participants. This is consistent with the initial design results.

Table 4 Improvement in AEP

Participant	Initial AEP	Optimal AEP	AEP Increase	Thrust Increase	Flapwise Bending Moment Increase
1	28.4 GWh	31.9 GWh	12.44%	13.98%	10.98%
2	28.7 GWh	31.3 GWh	9.20%	6.03%	1.63%
3 Fix	29.5 GWh	32.8 GWh	11.11%	12.65%	11.00%
3 Free	29.5 GWh	33.0 GWh	11.71%	9.95%	11.00%
4	29.2 GWh	32.3 GWh	10.49%	13.11%	10.95%
5	29.3 GWh	32.8 GWh	11.99%	13.78%	11.41%
6	29.3 GWh	32.2 GWh	10.11%	12.86%	11.00%
7	29.0 GWh	32.3 GWh	11.36%	12.86%	10.40%

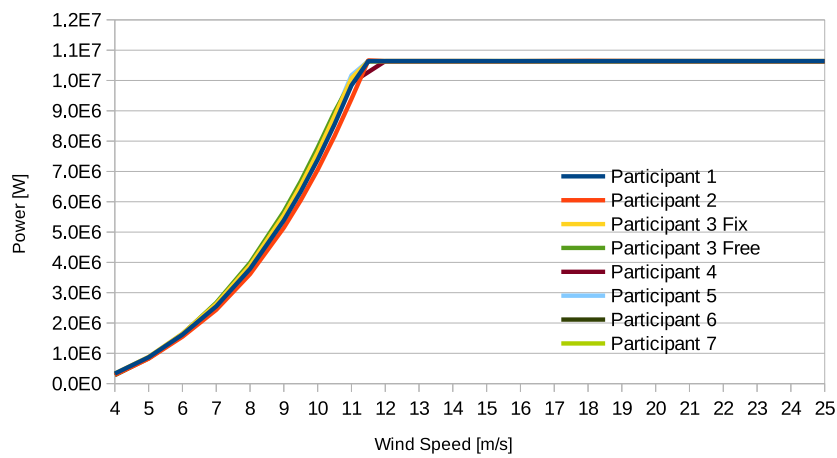


Fig. 12 The power of the optimal design

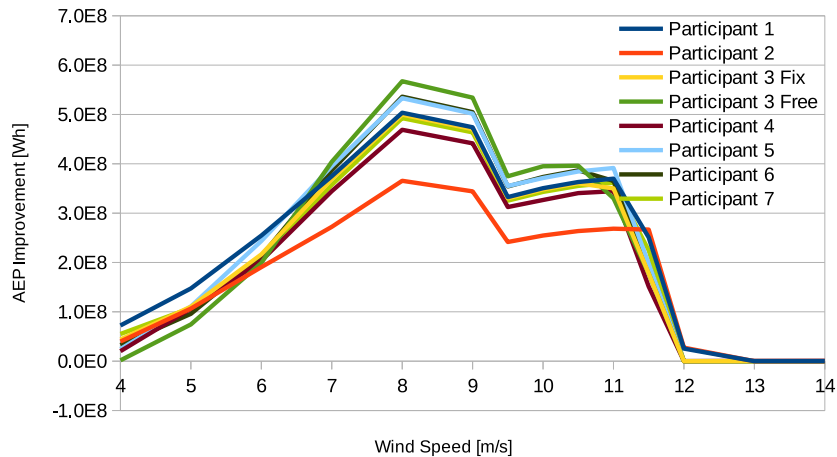


Fig. 13 The relative AEP of the optimal design

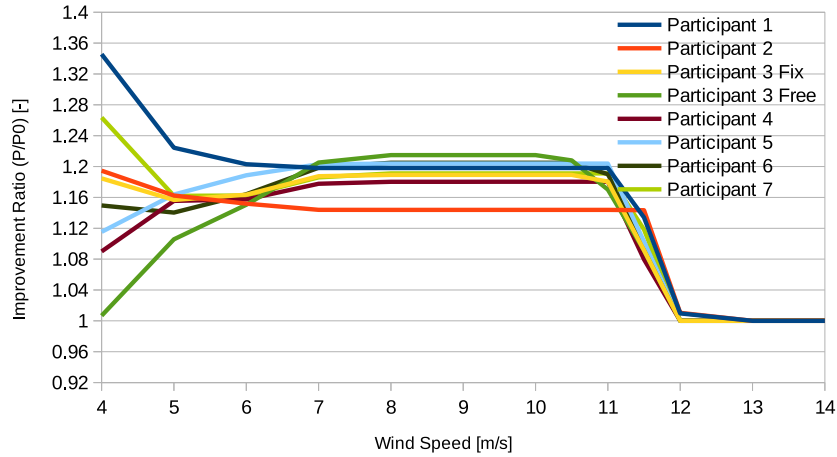


Fig. 14 The relative power of the optimal design

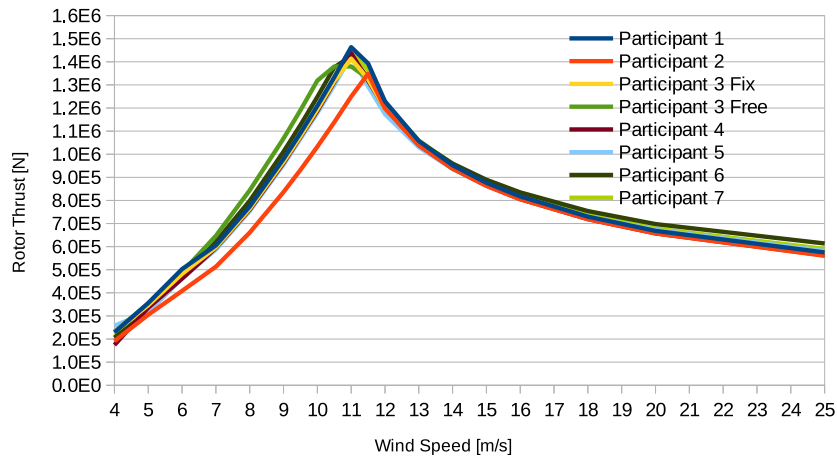


Fig. 15 The thrust of the optimal design

VI. Discussion

The ultimate goal of design optimization is to determine the design configuration that would result in the best performance. The fact that there was a wide range of differences in the design configurations shows that further work is needed to advance the field of numerical aerodynamic optimization for wind turbines. These differences can be explained by the test case itself, as the participants were free to choose their tools and optimization setup. This opens up a lot of different variables that could explain the differences seen here. However, this also shows the range of outcomes one could achieve using the different tools that are available, which is an indication of the maturity of aerodynamic design optimization in the research community. This further shows that more effort is needed to develop a better understanding of aerodynamic optimization and what leads to the differences shown here.

Optimization test cases are different from analysis test cases because there are three ways that the final results can vary. First, common to both types of test cases, is the differences in the predicted performance of different analysis codes for a common design. This will be referred to as Type I discrepancies. The analysis tool can introduce additional discrepancies, since it also defines the optimal design point that is being sought by the optimization. Thus, perfectly converged optimization can arrive to different points based on analysis differences as well. This will be referred to as a Type II discrepancy. The third set of differences is in the optimization algorithms employed by the different users, ultimately this is a matter of the degree of convergence that was achieved and where in the design space the optimization explored. This is referred to as a Type III discrepancy. These differences are shown schematically in Figure 17.

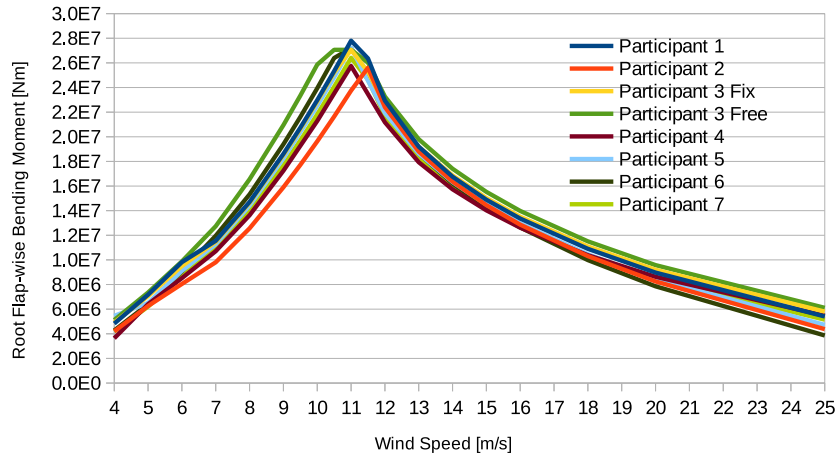


Fig. 16 The root flap-wise bending moment of the optimal design

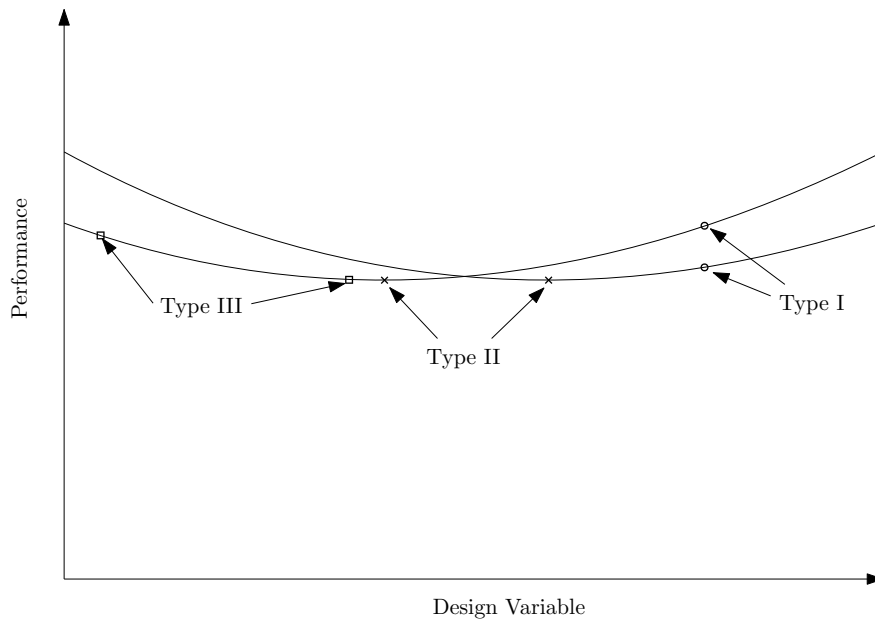


Fig. 17 Example of the types of discrepancies in the optimization test case

The relatively good agreement in the initial results (see Section IV) shows that the differences in the optimal designs cannot be attributed to Type I discrepancies alone. Yet, the freedom in the optimization test case makes it difficult to separate out Type II and Type III differences. Thus, we can only speculate on the sources of these differences and suggest future studies. It is likely that there are Type II discrepancies, as that the thrust constraint was only active for Participant I.

Type II discrepancies can potentially be explained by the BEM equations. The optimal power in the BEM equations is strongly defined by the overall loading [14]. This loading can be increased by increasing the chord and decreasing the twist. The results in Section V.A show that a high optimal chord corresponds to a high twist and vice versa. Thus, the different optimization solutions could be arriving at very similar loading levels. Once the loading level is fixed, the optimization is only varying the operating angle of attack. In this regime, the power is only affected by small changes in the lift to drag ratio (i.e. aerodynamic efficiency). Thus, the problem likely has a high degree of variation in design directions corresponding to changes in loading, while it has small variations in other directions. So the design problem may be flat in the direction of constant loading compared to directions that vary the loading. Figure 17 shows how

flatness could lead to large Type II discrepancies, despite Type I discrepancies being small. Thus, the relative flatness between these two design directions could make the BEM equations inherently sensitive to Type II discrepancies. When the design space is flat, large differences in the designs have a smaller impact on the performance and thrust. In this case, the differences shown in Section V.A are more acceptable.

Type I and II errors are explained by the analysis codes. These differences may be due to the different turbulent wake models, different tip loss functions and possibly different corrections to the airfoil data that were used by the participants. The impact of these different submodels on the optimal design has not been quantified, however the results here show some anecdotal evidence that differences in the analysis could explain some of the differences. For example, the wide variation in power improvement in the low wind speeds can be attributed to differences in the turbulent wake model. The large variations in design towards the tip and root of the blade could be attributed to different hub and tip loss models.

The effects of Type III discrepancies can manifest in two ways. First, the optimization problem could have multiple local minimum, and thus, different algorithms, perfectly converged, could lead to these different solutions. The optimization algorithm used by Participant 5 is less sensitive to local minimum; their optimal designs shows a larger chord and twist distributions and thinner airfoil sections than most of the other participants. At the same time, Participant 5 achieved a better performance than most participants. Furthermore, the design of Participant 5 is further from the initial design in the design space, thus, it is a possibility that the gradient-based results are getting trapped in a local minimum. Finally, the results of Participant 2 show that failing to converge can sacrifice 1–2% of potential improvement in AEP. Since the convergence of smooth convex optimization problems are based on the gradients of the problem, a very flat problem can also lead to large discrepancies due to different convergence tolerance and errors in the gradients.

Further information on Type I and II errors could be found by performing a cross comparison, where each of the participants simulated the solutions of the other participants. These calculations could not be completed in the time frame for this study.

Another source of discrepancy is in the relative maturity of the different optimization frameworks. Some of the participants in this study have a long history in numerical wind turbine design optimization, while others were actively developing their optimization tools during the study.

VII. Conclusions

An aerodynamic optimization test case was developed loosely based on the DTU 10-MW Reference Wind Turbine. The test case is purely aerodynamic, but thrust, moment and absolute thickness constraints indirectly introduced some structural aspects. To focus on the performance of the optimization, a maximum chord constraint was not used, leading to designs with chords too large to be relevant to industry.

Multiple institutes participated in this test case. A survey of the tools and optimization set-up showed that the greatest differences were more in the optimization algorithms than in the analysis. Yet, there were still differences in the analysis codes. The analysis of a fixed initial design did show some small differences in the predicted performance between the different analysis codes. Thus, differences in the analysis is a factor in these comparisons.

The different optimizations produced widely different optimal designs. This wide differences in the designs is problematic, since it shows that there is a large uncertainty in the solutions. The differences in the optimal performance was not as stark though. One explanation for this is that the design problem itself may be flat and that flatness could explain the differences. If the design problem is flat, the impact of large design differences is not as severe.

Since the users were free to choose any combination of analysis and optimization methods, there are many possible sources for these differences. Thus, it is difficult for this study to explain the differences in the results definitively. Neither differences in the analysis nor the optimization can be ruled out. The paper discusses three potential types of discrepancies and gives examples of how they could have manifested in this study. The different sources of discrepancies should be the focus of future investigations of numerical aerodynamic design optimization of wind turbines.

A. Test Case Data

To enable future research to use this test case, all the data for the test case are given here in tabular form. These data are given in Tables 5, 6, 7, 8, 9, 10, 11, 12, 13, 14, 15, 16, 17, 18, 19, 20 and 21.

Table 5 Initial planform design

<i>S</i>	<i>X</i>	<i>Y</i>	<i>Z</i>	Twist [deg]	Chord [m]	Lateral Shift [-]
0.00000	0.0	0.0	0.000	14.500	5.380	0.500
0.03057	0.0	0.0	2.643	14.500	5.380	0.500
0.06222	0.0	0.0	5.380	14.500	5.380	0.500
0.09487	0.0	0.0	8.203	14.445	5.474	0.494
0.12841	0.0	0.0	11.103	14.222	5.620	0.472
0.16274	0.0	0.0	14.071	13.727	5.727	0.440
0.19772	0.0	0.0	17.095	12.959	5.730	0.412
0.23321	0.0	0.0	20.164	12.078	5.630	0.391
0.26907	0.0	0.0	23.265	11.236	5.475	0.376
0.30515	0.0	0.0	26.384	10.476	5.325	0.365
0.34128	0.0	0.0	29.508	9.806	5.190	0.358
0.37731	0.0	0.0	32.623	9.206	5.044	0.353
0.41309	0.0	0.0	35.716	8.656	4.869	0.350
0.44846	0.0	0.0	38.773	8.102	4.676	0.350
0.48328	0.0	0.0	41.782	7.517	4.473	0.350
0.51741	0.0	0.0	44.732	6.916	4.263	0.350
0.55073	0.0	0.0	47.611	6.315	4.052	0.350
0.58312	0.0	0.0	50.410	5.727	3.844	0.350
0.61449	0.0	0.0	53.120	5.164	3.642	0.350
0.64476	0.0	0.0	55.734	4.635	3.449	0.350
0.67385	0.0	0.0	58.247	4.147	3.265	0.350
0.70172	0.0	0.0	60.653	3.701	3.093	0.350
0.72833	0.0	0.0	62.950	3.298	2.931	0.350
0.75364	0.0	0.0	65.135	2.935	2.780	0.350
0.77766	0.0	0.0	67.208	2.608	2.641	0.350
0.80038	0.0	0.0	69.167	2.314	2.512	0.350
0.82181	0.0	0.0	71.016	2.045	2.395	0.350
0.84197	0.0	0.0	72.755	1.797	2.286	0.350
0.86089	0.0	0.0	74.386	1.566	2.187	0.350
0.87861	0.0	0.0	75.913	1.350	2.097	0.350
0.89517	0.0	0.0	77.340	1.148	2.011	0.350
0.91061	0.0	0.0	78.671	0.959	1.925	0.350
0.92498	0.0	0.0	79.908	0.784	1.836	0.350
0.93833	0.0	0.0	81.059	0.625	1.741	0.350
0.95072	0.0	0.0	82.125	0.483	1.642	0.350
0.96220	0.0	0.0	83.113	0.358	1.532	0.350
0.97281	0.0	0.0	84.026	0.251	1.402	0.350
0.98262	0.0	0.0	84.870	0.157	1.294	0.350
0.99166	0.0	0.0	85.649	0.070	1.176	0.350
1.00000	0.0	0.0	86.366	0.000	1.035	0.350

Table 6 The blending weights for the airfoil coefficients

<i>S</i>	Cylinder	FFA-W3-600	FFA-W3-480	FFA-W3-360	FFA-W3-301	FFA-W3-241
0.00000	1.000					
0.03057	0.992	0.008				
0.06222	0.883	0.117				
0.09487	0.720	0.280				
0.12841	0.530	0.470				
0.16274	0.325	0.675				
0.19772	0.119	0.881				
0.23321		0.768	0.232			
0.26907		0.250	0.750			
0.30515			0.879	0.121		
0.34128			0.602	0.398		
0.37731			0.393	0.607		
0.41309			0.228	0.772		
0.44846			0.065	0.935		
0.48328				0.805	0.195	
0.51741				0.484	0.516	
0.55073				0.171	0.829	
0.58312					0.870	0.130
0.61449					0.545	0.455
0.64476					0.301	0.699
0.67385					0.146	0.854
0.70172					0.057	0.943
0.72833					0.014	0.986
0.75364						1.000
0.77766						1.000
0.80038						1.000
0.82181						1.000
0.84197						1.000
0.86089						1.000
0.87861						1.000
0.89517						1.000
0.91061						1.000
0.92498						1.000
0.93833						1.000
0.95072						1.000
0.96220						1.000
0.97281						1.000
0.98262						1.000
0.99166						1.000
1.00000						1.000

Table 7 The blending weights for the cross-section shape

<i>S</i>	Cylinder	TC72	FFA-W3-480	FFA-W3-360	FFA-W3-301	FFA-W3-241
0.00000	1.000					
0.03057	0.988	0.012				
0.06222	0.832	0.168				
0.09487	0.597	0.403				
0.12841	0.323	0.677				
0.16274	0.028	0.972				
0.19772		0.693	0.307			
0.23321		0.381	0.619			
0.26907		0.124	0.876			
0.30515			0.879	0.121		
0.34128			0.602	0.398		
0.37731			0.393	0.607		
0.41309			0.228	0.772		
0.44846			0.065	0.935		
0.48328				0.805	0.195	
0.51741				0.484	0.516	
0.55073				0.171	0.829	
0.58312					0.870	0.131
0.61449					0.545	0.455
0.64476					0.301	0.699
0.67385					0.146	0.854
0.70172					0.057	0.943
0.72833					0.014	0.986
0.75364						1.000
0.77766						1.000
0.80038						1.000
0.82181						1.000
0.84197						1.000
0.86089						1.000
0.87861						1.000
0.89517						1.000
0.91061						1.000
0.92498						1.000
0.93833						1.000
0.95072						1.000
0.96220						1.000
0.97281						1.000
0.98262						1.000
0.99166						1.000
1.00000						1.000

Table 8 The relative thickness of profiles shapes

Airfoil	Relative Thickness
FFA-W3-241	24.1%
FFA-W3-301	30.1%
FFA-W3-360	36.0%
FFA-W3-480	48.0%
FFA-W3-600	60.0%
TC72	72.0%
Cylinder	100.0%

Table 9 Airfoil coefficients for thin airfoils at negative angles of attack

AoA [deg]	FFA-W3-241			FFA-W3-301			FFA-W3-360		
	C_l	C_d	C_m	C_l	C_d	C_m	C_l	C_d	C_m
-180	0.0000	0.0000	0.0000	0.0000	0.0000	0.0000	0.0000	0.0000	0.0000
-175	0.1736	0.0114	0.0218	0.1736	0.0099	0.0218	0.1736	0.0099	0.0218
-170	0.3420	0.0452	0.0434	0.3420	0.0392	0.0434	0.3420	0.0392	0.0434
-165	0.5000	0.1005	0.0647	0.5000	0.0871	0.0647	0.5000	0.0871	0.0647
-160	0.6428	0.1755	0.0855	0.6428	0.1521	0.0855	0.6428	0.1521	0.0855
-155	0.7660	0.2679	0.1057	0.7660	0.2322	0.1057	0.7660	0.2322	0.1057
-150	0.8660	0.3750	0.1250	0.8660	0.3250	0.1250	0.8660	0.3250	0.1250
-145	0.9397	0.4935	0.1434	0.9397	0.4277	0.1434	0.9397	0.4277	0.1434
-140	0.9848	0.6197	0.1607	0.9848	0.5371	0.1607	0.9848	0.5371	0.1607
-135	1.0000	0.7500	0.1768	1.0000	0.6500	0.1768	1.0000	0.6500	0.1768
-130	0.9848	0.8803	0.1915	0.9848	0.7629	0.1915	0.9848	0.7629	0.1915
-125	0.9397	1.0065	0.2048	0.9397	0.8723	0.2048	0.9397	0.8723	0.2048
-120	0.8660	1.1250	0.2165	0.8660	0.9750	0.2165	0.8660	0.9750	0.2165
-115	0.7660	1.2321	0.2266	0.7660	1.0678	0.2266	0.7660	1.0678	0.2266
-110	0.6428	1.3245	0.2349	0.6428	1.1479	0.2349	0.6428	1.1479	0.2349
-105	0.5000	1.3995	0.2415	0.5000	1.2129	0.2415	0.5000	1.2129	0.2415
-100	0.3420	1.4548	0.2462	0.3420	1.2608	0.2462	0.3420	1.2608	0.2462
-95	0.1736	1.4886	0.2490	0.1736	1.2901	0.2490	0.1736	1.2901	0.2490
-90	0.0000	1.5000	0.2500	0.0000	1.3000	0.2500	0.0000	1.3000	0.2500
-85	-0.1736	1.4886	0.2490	-0.1736	1.2901	0.2490	-0.1736	1.2901	0.2490
-80	-0.3420	1.4548	0.2462	-0.3420	1.2608	0.2462	-0.3420	1.2608	0.2462
-75	-0.5000	1.3995	0.2415	-0.5000	1.2129	0.2415	-0.5000	1.2129	0.2415
-70	-0.6428	1.3245	0.2349	-0.6428	1.1479	0.2349	-0.6428	1.1479	0.2349
-65	-0.7660	1.2321	0.2266	-0.7660	1.0678	0.2266	-0.7660	1.0678	0.2266
-60	-0.8660	1.1250	0.2165	-0.8660	0.9750	0.2165	-0.8660	0.9750	0.2165
-55	-0.9397	1.0065	0.2048	-0.9397	0.8723	0.2048	-0.9397	0.8723	0.2048
-50	-0.9848	0.8603	0.1915	-0.9848	0.7629	0.1915	-0.9848	0.7629	0.1915
-45	-1.0120	0.7120	0.1708	-1.0000	0.6500	0.1768	-1.0000	0.6500	0.1768
-40	-1.0376	0.5475	0.1416	-1.0216	0.5352	0.1416	-0.9716	0.5352	0.1416
-39	-1.0419	0.5165	0.1346	-1.0239	0.5066	0.1346	-0.9639	0.5136	0.1346
-38	-1.0462	0.4816	0.1276	-1.0162	0.4851	0.1276	-0.9462	0.4851	0.1276
-37	-1.0525	0.4487	0.1185	-1.0185	0.4565	0.1205	-0.9285	0.4635	0.1205
-36	-1.0568	0.4177	0.1095	-1.0108	0.4279	0.1135	-0.9108	0.4349	0.1135
-35	-1.0611	0.3848	0.1005	-1.0031	0.3994	0.0965	-0.8931	0.4064	0.0965
-34	-1.0654	0.3558	0.0894	-0.9954	0.3708	0.0794	-0.8854	0.3778	0.0794
-33	-1.0717	0.3289	0.0824	-0.9877	0.3353	0.0624	-0.8677	0.3523	0.0624
-32	-1.0765	0.3031	0.0678	-0.9835	0.3097	0.0515	-0.8564	0.3315	0.0447
-30	-1.0889	0.2560	0.0508	-0.9703	0.2663	0.0389	-0.8378	0.2777	0.0327
-28	-1.0993	0.2090	0.0337	-0.9672	0.2229	0.0263	-0.8191	0.2338	0.0208
-26	-1.1168	0.1756	0.0206	-0.9441	0.1941	0.0154	-0.7924	0.2045	0.0102
-24	-1.1282	0.1423	0.0075	-0.9310	0.1654	0.0045	-0.7756	0.1751	-0.0004
-22	-1.1215	0.1183	-0.0008	-0.9047	0.1417	-0.0039	-0.7441	0.1513	-0.0089
-20	-1.1148	0.0943	-0.0091	-0.8784	0.1181	-0.0123	-0.7126	0.1274	-0.0174
-18	-1.0919	0.0765	-0.0123	-0.8459	0.0986	-0.0175	-0.6678	0.1085	-0.0229
-16	-1.0691	0.0587	-0.0156	-0.8134	0.0792	-0.0227	-0.6231	0.0896	-0.0285
-14	-1.0379	0.0454	-0.0156	-0.7728	0.0643	-0.0235	-0.5742	0.0748	-0.0300
-12	-1.0067	0.0321	-0.0155	-0.7322	0.0495	-0.0244	-0.5252	0.0600	-0.0314
-10	-0.8479	0.0230	-0.0318	-0.6935	0.0381	-0.0227	-0.4827	0.0485	-0.0279
-8	-0.6892	0.0138	-0.0480	-0.6547	0.0267	-0.0210	-0.4402	0.0370	-0.0244
-6	-0.4278	0.0118	-0.0611	-0.4507	0.0204	-0.0389	-0.2983	0.0294	-0.0359
-4	-0.1665	0.0098	-0.0742	-0.2467	0.0140	-0.0569	-0.1564	0.0219	-0.0474
-2	0.0863	0.0095	-0.0811	0.0295	0.0129	-0.0717	0.1744	0.0203	-0.0782

Table 10 Airfoil coefficients for thin airfoils at positive angles of attack

AoA [deg]	FFA-W3-241			FFA-W3-301			FFA-W3-360		
	C_l	C_d	C_m	C_l	C_d	C_m	C_l	C_d	C_m
0	0.3391	0.0092	-0.0880	0.3056	0.0118	-0.0865	0.5053	0.0187	-0.1090
2	0.5867	0.0094	-0.0933	0.5670	0.0119	-0.0954	0.8241	0.0188	-0.1329
4	0.8301	0.0099	-0.0977	0.8199	0.0125	-0.1024	1.1209	0.0196	-0.1510
6	1.0656	0.0109	-0.1008	1.0614	0.0136	-0.1071	1.3897	0.0213	-0.16298
8	1.2914	0.0124	-0.1026	1.2874	0.0152	-0.1094	1.6254	0.0240	-0.16908
10	1.5012	0.0144	-0.1024	1.4840	0.0180	-0.10796	1.8109	0.0279	-0.16832
12	1.6886	0.0173	-0.0998	1.6388	0.0224	-0.10256	1.8589	0.0365	-0.15848
14	1.8103	0.0226	-0.0941	1.7327	0.0303	-0.09524	1.8159	0.0760	-0.15576
16	1.8139	0.0354	-0.0874	1.7142	0.0539	-0.09104	1.7786	0.1165	-0.16696
18	1.7545	0.0647	-0.0850	1.6828	0.0954	-0.09794	1.7560	0.1571	-0.18094
20	1.6071	0.1035	-0.0913	1.6567	0.1435	-0.1103	1.7630	0.2063	-0.19598
22	1.5257	0.1437	-0.1026	1.6444	0.2280	-0.12996	1.8002	0.3057	-0.21428
24	1.4428	0.1841	-0.1140	1.6329	0.3148	-0.15332	1.8495	0.4153	-0.23648
26	1.3826	0.2290	-0.1282	1.6333	0.3926	-0.1760	1.8775	0.5163	-0.25882
28	1.3218	0.2738	-0.1423	1.6175	0.4623	-0.19658	1.8828	0.6069	-0.27966
30	1.2583	0.3278	-0.1582	1.5975	0.5266	-0.2149	1.8689	0.6892	-0.2983
32	1.1944	0.3816	-0.1739	1.5708	0.5855	-0.2313	1.8439	0.7625	-0.31466
33	1.1734	0.4209	-0.1790	1.5758	0.6215	-0.2366	1.8349	0.7954	-0.3166
34	1.1568	0.4504	-0.1831	1.5571	0.6562	-0.2406	1.8297	0.8232	-0.3106
35	1.1379	0.4815	-0.1873	1.5475	0.6897	-0.2447	1.8136	0.8446	-0.3047
36	1.1248	0.5105	-0.1914	1.5268	0.7148	-0.2487	1.7854	0.8684	-0.2987
37	1.1177	0.5450	-0.1953	1.5259	0.7464	-0.2496	1.7669	0.8912	-0.2926
38	1.1024	0.5737	-0.1993	1.5139	0.7762	-0.2455	1.7269	0.9066	-0.2865
39	1.0891	0.5999	-0.2032	1.4918	0.7982	-0.2444	1.6864	0.9255	-0.2844
40	1.0755	0.6280	-0.2071	1.4596	0.8197	-0.2423	1.6458	0.9385	-0.2803
45	1.0175	0.7578	-0.2161	1.2951	0.9122	-0.2373	1.4473	1.0290	-0.2633
50	0.9716	0.8820	-0.2184	1.1256	0.9665	-0.23537	1.1356	1.0715	-0.25437
55	0.9268	1.0104	-0.2214	0.9808	0.9957	-0.23243	0.9808	1.0857	-0.24543
60	0.8660	1.1250	-0.2255	0.8660	1.0350	-0.2335	0.8660	1.1000	-0.2365
65	0.7660	1.2321	-0.2306	0.7660	1.0828	-0.2336	0.7660	1.1278	-0.2366
70	0.6428	1.3245	-0.2349	0.6428	1.1479	-0.2349	0.6428	1.1629	-0.2389
75	0.5000	1.3995	-0.2415	0.5000	1.2129	-0.2415	0.5000	1.2129	-0.2415
80	0.3420	1.4548	-0.2462	0.3420	1.2608	-0.2462	0.3420	1.2608	-0.2462
85	0.1736	1.4886	-0.2490	0.1736	1.2901	-0.2490	0.1736	1.2901	-0.2490
90	0.0000	1.5000	-0.2500	0.0000	1.3000	-0.2500	0.0000	1.3000	-0.2500
95	-0.1736	1.4886	-0.2490	-0.1736	1.2901	-0.2490	-0.1736	1.2901	-0.2490
100	-0.3420	1.4548	-0.2462	-0.3420	1.2608	-0.2462	-0.3420	1.2608	-0.2462
105	-0.5000	1.3995	-0.2415	-0.5000	1.2129	-0.2415	-0.5000	1.2129	-0.2415
110	-0.6428	1.3245	-0.2349	-0.6428	1.1479	-0.2349	-0.6428	1.1479	-0.2349
115	-0.7660	1.2321	-0.2266	-0.7660	1.0678	-0.2266	-0.7660	1.0678	-0.2266
120	-0.8660	1.1250	-0.2165	-0.8660	0.9750	-0.2165	-0.8660	0.9750	-0.2165
125	-0.9397	1.0065	-0.2048	-0.9397	0.8723	-0.2048	-0.9397	0.8723	-0.2048
130	-0.9848	0.8803	-0.1915	-0.9848	0.7629	-0.1915	-0.9848	0.7629	-0.1915
135	-1.0000	0.7500	-0.1768	-1.0000	0.6500	-0.1768	-1.0000	0.6500	-0.1768
140	-0.9848	0.6197	-0.1607	-0.9848	0.5371	-0.1607	-0.9848	0.5371	-0.1607
145	-0.9397	0.4935	-0.1434	-0.9397	0.4277	-0.1434	-0.9397	0.4277	-0.1434
150	-0.8660	0.3750	-0.1250	-0.8660	0.3250	-0.1250	-0.8660	0.3250	-0.1250
155	-0.7660	0.2679	-0.1057	-0.7660	0.2322	-0.1057	-0.7660	0.2322	-0.1057
160	-0.6428	0.1755	-0.0855	-0.6428	0.1521	-0.0855	-0.6428	0.1521	-0.0855
165	-0.5000	0.1005	-0.0647	-0.5000	0.0871	-0.0647	-0.5000	0.0871	-0.0647
170	-0.3420	0.0452	-0.0434	-0.3420	0.0392	-0.0434	-0.3420	0.0392	-0.0434
175	-0.1736	0.0114	-0.0218	-0.1736	0.0099	-0.0218	-0.1736	0.0099	-0.0218
180	0.0000	0.0000	0.0000	0.0000	0.0000	0.0000	0.0000	0.0000	0.0000

Table 11 Airfoil coefficients for thick airfoils at negative angles of attack

AoA [deg]	FFA-W3-480			FFA-W3-600			Cylinder		
	C_l	C_d	C_m	C_l	C_d	C_m	C_l	C_d	C_m
-180	0.0000	0.0000	0.0000	0.0000	0.0000	0.0000	0.0000	0.6000	0.0000
-175	0.1736	0.0099	0.0218	0.1736	0.0099	0.0218	0.0000	0.6000	0.0000
-170	0.3420	0.0392	0.0434	0.3420	0.0392	0.0434	0.0000	0.6000	0.0000
-165	0.5000	0.0871	0.0647	0.5000	0.0871	0.0647	0.0000	0.6000	0.0000
-160	0.6428	0.1521	0.0855	0.6428	0.1521	0.0855	0.0000	0.6000	0.0000
-155	0.7660	0.2322	0.1057	0.7660	0.2322	0.1057	0.0000	0.6000	0.0000
-150	0.8660	0.3250	0.1250	0.8660	0.3250	0.1250	0.0000	0.6000	0.0000
-145	0.9397	0.4277	0.1434	0.9397	0.4277	0.1434	0.0000	0.6000	0.0000
-140	0.9848	0.5371	0.1607	0.9848	0.5371	0.1607	0.0000	0.6000	0.0000
-135	1.0000	0.6500	0.1768	1.0000	0.6500	0.1768	0.0000	0.6000	0.0000
-130	0.9848	0.7629	0.1915	0.9848	0.7629	0.1915	0.0000	0.6000	0.0000
-125	0.9397	0.8723	0.2048	0.9397	0.8723	0.2048	0.0000	0.6000	0.0000
-120	0.8660	0.9750	0.2165	0.8660	0.9750	0.2165	0.0000	0.6000	0.0000
-115	0.7660	1.0678	0.2266	0.7660	1.0678	0.2266	0.0000	0.6000	0.0000
-110	0.6428	1.1479	0.2349	0.6428	1.1479	0.2349	0.0000	0.6000	0.0000
-105	0.5000	1.2129	0.2415	0.5000	1.2129	0.2415	0.0000	0.6000	0.0000
-100	0.3420	1.2608	0.2462	0.3420	1.2608	0.2462	0.0000	0.6000	0.0000
-95	0.1736	1.2901	0.2490	0.1736	1.2901	0.2490	0.0000	0.6000	0.0000
-90	0.0000	1.3000	0.2500	0.0000	1.3000	0.2500	0.0000	0.6000	0.0000
-85	-0.1736	1.2901	0.2490	-0.1736	1.2901	0.2490	0.0000	0.6000	0.0000
-80	-0.3420	1.2608	0.2462	-0.3420	1.2608	0.2462	0.0000	0.6000	0.0000
-75	-0.5000	1.2129	0.2415	-0.5000	1.2129	0.2415	0.0000	0.6000	0.0000
-70	-0.6428	1.1479	0.2349	-0.6428	1.1479	0.2349	0.0000	0.6000	0.0000
-65	-0.7660	1.0678	0.2266	-0.7660	1.0678	0.2266	0.0000	0.6000	0.0000
-60	-0.8660	0.9750	0.2165	-0.8660	0.9750	0.2165	0.0000	0.6000	0.0000
-55	-0.9397	0.8723	0.1978	-0.9397	0.8723	0.1978	0.0000	0.6000	0.0000
-50	-0.9848	0.7629	0.1775	-0.9848	0.7629	0.1775	0.0000	0.6000	0.0000
-45	-1.0000	0.6500	0.1558	-1.0000	0.6500	0.1488	0.0000	0.6000	0.0000
-40	-0.9816	0.5352	0.1246	-0.9516	0.5282	0.1176	0.0000	0.6000	0.0000
-39	-0.9539	0.5136	0.1106	-0.9039	0.5026	0.1076	0.0000	0.6000	0.0000
-38	-0.9262	0.4851	0.0966	-0.8262	0.4671	0.0906	0.0000	0.6000	0.0000
-37	-0.8885	0.4565	0.0825	-0.7185	0.4345	0.0805	0.0000	0.6000	0.0000
-36	-0.8508	0.4279	0.0655	-0.6208	0.3989	0.0665	0.0000	0.6000	0.0000
-35	-0.8231	0.3924	0.0585	-0.5231	0.3634	0.0595	0.0000	0.6000	0.0000
-34	-0.7854	0.3638	0.0484	-0.4454	0.3278	0.0524	0.0000	0.6000	0.0000
-33	-0.7477	0.3383	0.0384	-0.3477	0.3013	0.0454	0.0000	0.6000	0.0000
-32	-0.7011	0.3123	0.0305	-0.2571	0.2729	0.04699	0.0000	0.6000	0.0000
-30	-0.6208	0.2663	0.0200	-0.1574	0.2332	0.0606	0.0000	0.6000	0.0000
-28	-0.5406	0.2402	0.0094	-0.0776	0.2034	0.0742	0.0000	0.6000	0.0000
-26	-0.4694	0.2169	-0.0006	0.0115	0.1858	0.08749	0.0000	0.6000	0.0000
-24	-0.3881	0.1936	-0.0106	0.1007	0.1681	0.10079	0.0000	0.6000	0.0000
-22	-0.3161	0.1732	-0.0197	0.1962	0.1526	0.11329	0.0000	0.6000	0.0000
-20	-0.2442	0.1529	-0.0289	0.2918	0.1370	0.12579	0.0000	0.6000	0.0000
-18	-0.1641	0.1355	-0.0368	0.3932	0.1240	0.1370	0.0000	0.6000	0.0000
-16	-0.0841	0.1180	-0.0448	0.4947	0.1109	0.14822	0.0000	0.6000	0.0000
-14	0.0021	0.1035	-0.0510	0.6004	0.1009	0.15711	0.0000	0.6000	0.0000
-12	0.0883	0.0890	-0.0572	0.7061	0.0908	0.1660	0.0000	0.6000	0.0000
-10	0.1722	0.0773	-0.0604	0.7880	0.0836	0.16771	0.0000	0.6000	0.0000
-8	0.2561	0.0656	-0.0636	0.8700	0.0765	0.16942	0.0000	0.6000	0.0000
-6	0.3179	0.0563	-0.0605	0.8358	0.0748	-0.1470	0.0000	0.6000	0.0000
-4	0.3798	0.0470	-0.0574	0.8162	0.07311	-0.12588	0.0000	0.6000	0.0000
-2	0.3573	0.0405	-0.0351	0.6603	0.07553	-0.08764	0.0000	0.6000	0.0000

Table 12 Airfoil coefficients for thick airfoils at positive angles of attack

AoA [deg]	FFA-W3-480			FFA-W3-600			Cylinder		
	C_l	C_d	C_m	C_l	C_d	C_m	C_l	C_d	C_m
0	0.3348	0.0341	-0.0128	0.5199	0.07795	-0.05062	0.0000	0.6000	0.0000
2	0.5652	0.0316	-0.0494	0.2636	0.07795	-0.00078	0.0000	0.6000	0.0000
4	0.8769	0.0343	-0.0894	0.2146	0.07082	0.06962	0.0000	0.6000	0.0000
6	1.0425	0.0451	-0.11168	0.1656	0.07483	0.01974	0.0000	0.6000	0.0000
8	0.9487	0.0700	-0.12084	0.4475	0.08587	-0.02718	0.0000	0.6000	0.0000
10	0.9088	0.0886	-0.1376	0.7071	0.0999	-0.06712	0.0000	0.6000	0.0000
12	0.9761	0.0993	-0.15942	0.9540	0.11148	-0.10334	0.0000	0.6000	0.0000
14	1.1130	0.1070	-0.18234	1.1891	0.12072	-0.13694	0.0000	0.6000	0.0000
16	1.3065	0.1163	-0.20664	1.4183	0.13678	-0.16866	0.0000	0.6000	0.0000
18	1.5414	0.1317	-0.2315	1.6392	0.14998	-0.19886	0.0000	0.6000	0.0000
20	1.8049	0.1570	-0.25662	1.8216	0.16894	-0.22524	0.0000	0.6000	0.0000
22	2.0020	0.2757	-0.28058	1.9837	0.20657	-0.25094	0.0000	0.6000	0.0000
24	2.1216	0.4224	-0.30574	2.0985	0.30919	-0.27474	0.0000	0.6000	0.0000
26	2.1916	0.5610	-0.3294	2.1904	0.4344	-0.29658	0.0000	0.6000	0.0000
28	2.2291	0.6861	-0.35198	2.2541	0.5512	-0.31712	0.0000	0.6000	0.0000
30	2.2322	0.7958	-0.3710	2.2731	0.6732	-0.33352	0.0000	0.6000	0.0000
32	2.2188	0.8915	-0.38784	2.2740	0.7756	-0.34854	0.0000	0.6000	0.0000
33	2.2092	0.9229	-0.3845	2.2780	0.8209	-0.3466	0.0000	0.6000	0.0000
34	2.1927	0.9472	-0.3806	2.2658	0.8551	-0.3476	0.0000	0.6000	0.0000
35	2.1625	0.9664	-0.3747	2.2408	0.8862	-0.3487	0.0000	0.6000	0.0000
36	2.1313	0.9889	-0.3687	2.2331	0.9141	-0.3427	0.0000	0.6000	0.0000
37	2.0878	1.0073	-0.3626	2.2134	0.9390	-0.3366	0.0000	0.6000	0.0000
38	2.0435	1.0284	-0.3565	2.1820	0.9709	-0.3305	0.0000	0.6000	0.0000
39	1.9984	1.0521	-0.3504	2.1391	0.9996	-0.3244	0.0000	0.6000	0.0000
40	1.9418	1.0769	-0.3443	2.0951	1.0254	-0.3183	0.0000	0.6000	0.0000
45	1.6535	1.1697	-0.3233	1.8370	1.1419	-0.3003	0.0000	0.6000	0.0000
50	1.3016	1.1965	-0.30437	1.5156	1.1615	-0.29137	0.0000	0.6000	0.0000
55	1.0308	1.1957	-0.29543	1.2008	1.1657	-0.28243	0.0000	0.6000	0.0000
60	0.8660	1.1900	-0.2865	0.9660	1.1750	-0.2735	0.0000	0.6000	0.0000
65	0.7660	1.1928	-0.2766	0.7660	1.1778	-0.2636	0.0000	0.6000	0.0000
70	0.6428	1.2029	-0.2649	0.6428	1.1979	-0.2549	0.0000	0.6000	0.0000
75	0.5000	1.2129	-0.2515	0.5000	1.2129	-0.2515	0.0000	0.6000	0.0000
80	0.3420	1.2608	-0.2462	0.3420	1.2608	-0.2462	0.0000	0.6000	0.0000
85	0.1736	1.2901	-0.2490	0.1736	1.2901	-0.2490	0.0000	0.6000	0.0000
90	0.0000	1.3000	-0.2500	0.0000	1.3000	-0.2500	0.0000	0.6000	0.0000
95	-0.1736	1.2901	-0.2490	-0.1736	1.2901	-0.2490	0.0000	0.6000	0.0000
100	-0.3420	1.2608	-0.2462	-0.3420	1.2608	-0.2462	0.0000	0.6000	0.0000
105	-0.5000	1.2129	-0.2415	-0.5000	1.2129	-0.2415	0.0000	0.6000	0.0000
110	-0.6428	1.1479	-0.2349	-0.6428	1.1479	-0.2349	0.0000	0.6000	0.0000
115	-0.7660	1.0678	-0.2266	-0.7660	1.0678	-0.2266	0.0000	0.6000	0.0000
120	-0.8660	0.9750	-0.2165	-0.8660	0.9750	-0.2165	0.0000	0.6000	0.0000
125	-0.9397	0.8723	-0.2048	-0.9397	0.8723	-0.2048	0.0000	0.6000	0.0000
130	-0.9848	0.7629	-0.1915	-0.9848	0.7629	-0.1915	0.0000	0.6000	0.0000
135	-1.0000	0.6500	-0.1768	-1.0000	0.6500	-0.1768	0.0000	0.6000	0.0000
140	-0.9848	0.5371	-0.1607	-0.9848	0.5371	-0.1607	0.0000	0.6000	0.0000
145	-0.9397	0.4277	-0.1434	-0.9397	0.4277	-0.1434	0.0000	0.6000	0.0000
150	-0.8660	0.3250	-0.1250	-0.8660	0.3250	-0.1250	0.0000	0.6000	0.0000
155	-0.7660	0.2322	-0.1057	-0.7660	0.2322	-0.1057	0.0000	0.6000	0.0000
160	-0.6428	0.1521	-0.0855	-0.6428	0.1521	-0.0855	0.0000	0.6000	0.0000
165	-0.5000	0.0871	-0.0647	-0.5000	0.0871	-0.0647	0.0000	0.6000	0.0000
170	-0.3420	0.0392	-0.0434	-0.3420	0.0392	-0.0434	0.0000	0.6000	0.0000
175	-0.1736	0.0099	-0.0218	-0.1736	0.0099	-0.0218	0.0000	0.6000	0.0000
180	0.0000	0.0000	0.0000	0.0000	0.0000	0.0000	0.0000	0.6000	0.0000

Table 13 FFA-W3-241 cross section shape coordinates

ID	s	x	y	ID	s	x	y
1	0.00000	1.00000	-0.00360	41	0.50369	0.00130	0.00956
2	0.00794	0.98338	-0.00140	42	0.50897	0.00507	0.02005
3	0.01692	0.96457	0.00096	43	0.51468	0.01133	0.03033
4	0.02689	0.94365	0.00311	44	0.52116	0.02006	0.04087
5	0.03778	0.92072	0.00466	45	0.52841	0.03122	0.05135
6	0.04954	0.89589	0.00528	46	0.53648	0.04474	0.06170
7	0.06215	0.86928	0.00473	47	0.54536	0.06056	0.07176
8	0.07557	0.84102	0.00291	48	0.55506	0.07861	0.08139
9	0.08976	0.81124	-0.00030	49	0.56554	0.09880	0.09044
10	0.10469	0.78010	-0.00514	50	0.57678	0.12104	0.09873
11	0.12036	0.74772	-0.01183	51	0.58876	0.14522	0.10613
12	0.13669	0.71428	-0.02024	52	0.60144	0.17121	0.11247
13	0.15363	0.67994	-0.03015	53	0.61479	0.19891	0.11764
14	0.17107	0.64485	-0.04127	54	0.62877	0.22817	0.12153
15	0.18887	0.60918	-0.05308	55	0.64336	0.25885	0.12409
16	0.20687	0.57311	-0.06502	56	0.65851	0.29081	0.12526
17	0.22491	0.53681	-0.07651	57	0.67418	0.32389	0.12504
18	0.24285	0.50045	-0.08706	58	0.69033	0.35794	0.12350
19	0.26055	0.46422	-0.09623	59	0.70690	0.39279	0.12076
20	0.27795	0.42827	-0.10370	60	0.72380	0.42827	0.11696
21	0.29497	0.39279	-0.10938	61	0.74098	0.46422	0.11223
22	0.31158	0.35794	-0.11324	62	0.75834	0.50045	0.10670
23	0.32775	0.32389	-0.11531	63	0.77582	0.53681	0.10052
24	0.34342	0.29081	-0.11567	64	0.79331	0.57311	0.09382
25	0.35857	0.25885	-0.11441	65	0.81072	0.60918	0.08672
26	0.37317	0.22817	-0.11167	66	0.82798	0.64485	0.07935
27	0.38717	0.19891	-0.10754	67	0.84498	0.67994	0.07187
28	0.40054	0.17121	-0.10213	68	0.86163	0.71428	0.06441
29	0.41324	0.14522	-0.09560	69	0.87785	0.74772	0.05707
30	0.42523	0.12104	-0.08811	70	0.89355	0.78010	0.04996
31	0.43647	0.09880	-0.07985	71	0.90866	0.81124	0.04316
32	0.44691	0.07861	-0.07104	72	0.92309	0.84102	0.03673
33	0.45650	0.06056	-0.06188	73	0.93678	0.86928	0.03070
34	0.46519	0.04474	-0.05258	74	0.94966	0.89589	0.02510
35	0.47295	0.03122	-0.04334	75	0.96168	0.92072	0.01996
36	0.47976	0.02006	-0.03427	76	0.97276	0.94365	0.01529
37	0.48562	0.01133	-0.02550	77	0.98287	0.96457	0.01107
38	0.49063	0.00507	-0.01700	78	0.99197	0.98338	0.00727
39	0.49480	0.00130	-0.00903	79	1.00000	1.00000	0.00391
40	0.49987	0.00004	0.00160				

Table 14 FFA-W3-301 cross section shape coordinates

ID	s	x	y	ID	s	x	y
1	0.00000	1.00000	-0.00891	41	0.50771	0.00126	0.01326
2	0.00783	0.98338	-0.00558	42	0.51414	0.00503	0.02667
3	0.01662	0.96457	-0.00261	43	0.52095	0.01130	0.04001
4	0.02634	0.94364	-0.00051	44	0.52833	0.02003	0.05339
5	0.03694	0.92071	0.00058	45	0.53629	0.03118	0.06655
6	0.04841	0.89588	0.00040	46	0.54490	0.04470	0.07938
7	0.06072	0.86927	-0.00134	47	0.55415	0.06052	0.09167
8	0.07387	0.84101	-0.00479	48	0.56406	0.07858	0.10323
9	0.08783	0.81124	-0.01002	49	0.57459	0.09877	0.11385
10	0.10259	0.78009	-0.01715	50	0.58576	0.12101	0.12332
11	0.11813	0.74772	-0.02631	51	0.59754	0.14518	0.13146
12	0.13438	0.71428	-0.03722	52	0.60994	0.17118	0.13814
13	0.15125	0.67993	-0.04966	53	0.62294	0.19888	0.14325
14	0.16862	0.64484	-0.06318	54	0.63655	0.22813	0.14673
15	0.18632	0.60917	-0.07722	55	0.65075	0.25882	0.14866
16	0.20418	0.57310	-0.09116	56	0.66551	0.29078	0.14908
17	0.22203	0.53680	-0.10442	57	0.68080	0.32386	0.14807
18	0.23973	0.50044	-0.11652	58	0.69656	0.35791	0.14578
19	0.25716	0.46420	-0.12710	59	0.71274	0.39276	0.14230
20	0.27426	0.42824	-0.13591	60	0.72926	0.42824	0.13776
21	0.29095	0.39276	-0.14283	61	0.74605	0.46420	0.13229
22	0.30721	0.35791	-0.14780	62	0.76304	0.50044	0.12601
23	0.32300	0.32386	-0.15080	63	0.78013	0.53680	0.11909
24	0.33829	0.29078	-0.15188	64	0.79724	0.57310	0.11169
25	0.35305	0.25882	-0.15108	65	0.81428	0.60917	0.10391
26	0.36728	0.22813	-0.14847	66	0.83117	0.64484	0.09587
27	0.38093	0.19888	-0.14411	67	0.84782	0.67993	0.08766
28	0.39403	0.17118	-0.13810	68	0.86413	0.71428	0.07939
29	0.40653	0.14518	-0.13052	69	0.88004	0.74772	0.07116
30	0.41844	0.12101	-0.12155	70	0.89545	0.78009	0.06309
31	0.42974	0.09877	-0.11136	71	0.91028	0.81124	0.05528
32	0.44040	0.07858	-0.10018	72	0.92445	0.84101	0.04780
33	0.45039	0.06052	-0.08825	73	0.93791	0.86927	0.04074
34	0.45969	0.04470	-0.07582	74	0.95057	0.89588	0.03417
35	0.46825	0.03118	-0.06312	75	0.96237	0.92071	0.02812
36	0.47608	0.02003	-0.05035	76	0.97326	0.94364	0.02266
37	0.48320	0.01130	-0.03764	77	0.98319	0.96457	0.01775
38	0.48971	0.00503	-0.02502	78	0.99211	0.98338	0.01333
39	0.49573	0.00126	-0.01256	79	1.00000	1.00000	0.00937
40	0.50101	0.00000	-0.00119				

Table 15 FFA-W3-360 cross section shape coordinates

ID	s	x	y	ID	s	x	y
1	0.00000	1.00000	-0.01393	41	0.50753	0.00138	0.01755
2	0.00773	0.98339	-0.00928	42	0.51835	0.00515	0.04140
3	0.01633	0.96457	-0.00555	43	0.52693	0.01141	0.05950
4	0.02575	0.94365	-0.00342	44	0.53576	0.02014	0.07716
5	0.03603	0.92072	-0.00273	45	0.54482	0.03126	0.09405
6	0.04716	0.89589	-0.00361	46	0.55420	0.04481	0.11001
7	0.05914	0.86929	-0.00636	47	0.56389	0.06063	0.12474
8	0.07199	0.84103	-0.01120	48	0.57393	0.07868	0.13804
9	0.08569	0.81126	-0.01816	49	0.58441	0.09887	0.14982
10	0.10022	0.78011	-0.02713	50	0.59536	0.12111	0.15996
11	0.11553	0.74774	-0.03807	51	0.60684	0.14528	0.16844
12	0.13156	0.71431	-0.05083	52	0.61887	0.17128	0.17512
13	0.14821	0.67996	-0.06500	53	0.63146	0.19897	0.17994
14	0.16531	0.64487	-0.08000	54	0.64464	0.22823	0.18291
15	0.18269	0.60921	-0.09522	55	0.65840	0.25891	0.18414
16	0.20017	0.57314	-0.11009	56	0.67272	0.29086	0.18370
17	0.21761	0.53685	-0.12416	57	0.68757	0.32394	0.18171
18	0.23490	0.50049	-0.13705	58	0.70290	0.35799	0.17825
19	0.25192	0.46426	-0.14848	59	0.71866	0.39283	0.17347
20	0.26860	0.42831	-0.15816	60	0.73478	0.42831	0.16749
21	0.28486	0.39283	-0.16578	61	0.75120	0.46426	0.16048
22	0.30067	0.35799	-0.17134	62	0.76781	0.50049	0.15262
23	0.31601	0.32394	-0.17488	63	0.78454	0.53685	0.14408
24	0.33085	0.29086	-0.17643	64	0.80130	0.57314	0.13505
25	0.34517	0.25891	-0.17603	65	0.81800	0.60921	0.12568
26	0.35896	0.22823	-0.17375	66	0.83454	0.64487	0.11611
27	0.37219	0.19897	-0.16970	67	0.85085	0.67996	0.10647
28	0.38486	0.17128	-0.16402	68	0.86683	0.71431	0.09687
29	0.39695	0.14528	-0.15683	69	0.88240	0.74774	0.08740
30	0.40845	0.12111	-0.14818	70	0.89749	0.78011	0.07815
31	0.41937	0.09887	-0.13821	71	0.91201	0.81126	0.06920
32	0.42973	0.07868	-0.12695	72	0.92589	0.84103	0.06063
33	0.43958	0.06063	-0.11440	73	0.93907	0.86929	0.05251
34	0.44898	0.04481	-0.10064	74	0.95147	0.89589	0.04489
35	0.45796	0.03126	-0.08587	75	0.96303	0.92072	0.03783
36	0.46662	0.02014	-0.07006	76	0.97371	0.94365	0.03137
37	0.47509	0.01141	-0.05330	77	0.98345	0.96457	0.02543
38	0.48323	0.00515	-0.03624	78	0.99223	0.98339	0.01997
39	0.49308	0.00138	-0.01459	79	1.00000	1.00000	0.01503
40	0.50237	0.00012	0.00612				

Table 16 FFA-W3-480 cross section shape coordinates

ID	s	x	y	ID	s	x	y
1	0.00000	1.00000	-0.01857	41	0.51000	0.00138	0.02340
2	0.00752	0.98339	-0.01237	42	0.52358	0.00515	0.05520
3	0.01577	0.96457	-0.00740	43	0.53415	0.01141	0.07933
4	0.02472	0.94365	-0.00456	44	0.54479	0.02014	0.10288
5	0.03445	0.92072	-0.00364	45	0.55544	0.03126	0.12540
6	0.04499	0.89589	-0.00481	46	0.56614	0.04481	0.14668
7	0.05637	0.86929	-0.00848	47	0.57683	0.06063	0.16632
8	0.06866	0.84103	-0.01493	48	0.58756	0.07868	0.18405
9	0.08188	0.81126	-0.02421	49	0.59840	0.09887	0.19976
10	0.09603	0.78011	-0.03617	50	0.60944	0.12111	0.21328
11	0.11108	0.74774	-0.05076	51	0.62075	0.14528	0.22459
12	0.12698	0.71431	-0.06777	52	0.63240	0.17128	0.23349
13	0.14361	0.67996	-0.08667	53	0.64445	0.19897	0.23992
14	0.16073	0.64487	-0.10667	54	0.65697	0.22823	0.24388
15	0.17812	0.60921	-0.12696	55	0.67000	0.25891	0.24552
16	0.19557	0.57314	-0.14679	56	0.68354	0.29086	0.24493
17	0.21289	0.53685	-0.16555	57	0.69761	0.32394	0.24228
18	0.22994	0.50049	-0.18273	58	0.71218	0.35799	0.23767
19	0.24661	0.46426	-0.19797	59	0.72720	0.39283	0.23129
20	0.26280	0.42831	-0.21088	60	0.74261	0.42831	0.22332
21	0.27845	0.39283	-0.22104	61	0.75836	0.46426	0.21397
22	0.29355	0.35799	-0.22845	62	0.77435	0.50049	0.20349
23	0.30812	0.32394	-0.23317	63	0.79051	0.53685	0.19211
24	0.32218	0.29086	-0.23524	64	0.80672	0.57314	0.18007
25	0.33572	0.25891	-0.23471	65	0.82290	0.60921	0.16757
26	0.34880	0.22823	-0.23167	66	0.83896	0.64487	0.15481
27	0.36141	0.19897	-0.22627	67	0.85480	0.67996	0.14196
28	0.37358	0.17128	-0.21869	68	0.87034	0.71431	0.12916
29	0.38533	0.14528	-0.20911	69	0.88549	0.74774	0.11653
30	0.39668	0.12111	-0.19757	70	0.90018	0.78011	0.10420
31	0.40767	0.09887	-0.18428	71	0.91432	0.81126	0.09227
32	0.41834	0.07868	-0.16927	72	0.92784	0.84103	0.08084
33	0.42877	0.06063	-0.15253	73	0.94067	0.86929	0.07001
34	0.43904	0.04481	-0.13419	74	0.95274	0.89589	0.05985
35	0.44918	0.03126	-0.11449	75	0.96400	0.92072	0.05044
36	0.45928	0.02014	-0.09341	76	0.97439	0.94365	0.04183
37	0.46945	0.01141	-0.07107	77	0.98387	0.96457	0.03391
38	0.47945	0.00515	-0.04832	78	0.99242	0.98339	0.02663
39	0.49180	0.00138	-0.01945	79	1.00000	1.00000	0.02004
40	0.50352	0.00012	0.00816				

Table 17 TC-72 cross section shape coordinates, Part 1

ID	s	x	y	ID	s	x	y	ID	s	x	y
1	0.00000	0.99937	-0.02908	51	0.24835	0.44713	-0.35336	101	0.44384	0.02643	-0.13282
2	0.00491	0.98757	-0.03411	52	0.25292	0.43529	-0.35489	102	0.44693	0.02343	-0.12533
3	0.00986	0.97569	-0.03922	53	0.25746	0.42347	-0.35608	103	0.44998	0.02065	-0.11786
4	0.01487	0.96410	-0.04534	54	0.26199	0.41168	-0.35694	104	0.45300	0.01807	-0.11041
5	0.01992	0.95277	-0.05209	55	0.26649	0.39993	-0.35747	105	0.45599	0.01569	-0.10298
6	0.02500	0.94160	-0.05923	56	0.27097	0.38822	-0.35768	106	0.45894	0.01350	-0.09560
7	0.03009	0.93059	-0.06672	57	0.27543	0.37658	-0.35756	107	0.46185	0.01149	-0.08825
8	0.03521	0.91973	-0.07449	58	0.27986	0.36500	-0.35714	108	0.46473	0.00964	-0.08095
9	0.04033	0.90900	-0.08251	59	0.28427	0.35350	-0.35642	109	0.46758	0.00796	-0.07371
10	0.04543	0.89851	-0.09073	60	0.28866	0.34208	-0.35541	110	0.47039	0.00646	-0.06651
11	0.05048	0.88835	-0.09911	61	0.29302	0.33076	-0.35411	111	0.47317	0.00515	-0.05936
12	0.05553	0.87826	-0.10761	62	0.29736	0.31954	-0.35251	112	0.47592	0.00404	-0.05227
13	0.06058	0.86822	-0.11619	63	0.30167	0.30843	-0.35063	113	0.47864	0.00312	-0.04524
14	0.06564	0.85821	-0.12481	64	0.30596	0.29744	-0.34847	114	0.48132	0.00234	-0.03828
15	0.07070	0.84819	-0.13345	65	0.31023	0.28658	-0.34602	115	0.48397	0.00169	-0.03139
16	0.07577	0.83815	-0.14208	66	0.31446	0.27585	-0.34330	116	0.48658	0.00115	-0.02457
17	0.08084	0.82809	-0.15069	67	0.31867	0.26526	-0.34031	117	0.48917	0.00069	-0.01783
18	0.08591	0.81800	-0.15927	68	0.32286	0.25482	-0.33705	118	0.49172	0.00033	-0.01117
19	0.09098	0.80787	-0.16782	69	0.32702	0.24455	-0.33354	119	0.49425	0.00010	-0.00458
20	0.09605	0.79770	-0.17630	70	0.33115	0.23444	-0.32977	120	0.49674	0.00002	0.00193
21	0.10112	0.78747	-0.18472	71	0.33525	0.22450	-0.32576	121	0.49924	0.00010	0.00845
22	0.10619	0.77719	-0.19307	72	0.33932	0.21473	-0.32151	122	0.50176	0.00038	0.01504
23	0.11126	0.76684	-0.20131	73	0.34337	0.20516	-0.31703	123	0.50431	0.00078	0.02168
24	0.11632	0.75641	-0.20945	74	0.34739	0.19576	-0.31234	124	0.50689	0.00125	0.02842
25	0.12138	0.74590	-0.21747	75	0.35141	0.18649	-0.30743	125	0.50951	0.00179	0.03524
26	0.12643	0.73532	-0.22536	76	0.35539	0.17742	-0.30233	126	0.51216	0.00241	0.04214
27	0.13148	0.72464	-0.23310	77	0.35934	0.16858	-0.29702	127	0.51485	0.00316	0.04911
28	0.13652	0.71388	-0.24069	78	0.36325	0.15995	-0.29154	128	0.51756	0.00405	0.05615
29	0.14156	0.70302	-0.24812	79	0.36713	0.15154	-0.28588	129	0.52031	0.00511	0.06325
30	0.14658	0.69207	-0.25537	80	0.37098	0.14335	-0.28005	130	0.52309	0.00636	0.07041
31	0.15160	0.68104	-0.26244	81	0.37479	0.13540	-0.27406	131	0.52591	0.00782	0.07762
32	0.15661	0.66991	-0.26931	82	0.37857	0.12768	-0.26791	132	0.52876	0.00945	0.08488
33	0.16161	0.65868	-0.27599	83	0.38231	0.12019	-0.26161	133	0.53164	0.01125	0.09219
34	0.16659	0.64737	-0.28245	84	0.38602	0.11294	-0.25517	134	0.53455	0.01321	0.09955
35	0.17157	0.63596	-0.28870	85	0.38970	0.10593	-0.24861	135	0.53750	0.01533	0.10696
36	0.17654	0.62447	-0.29471	86	0.39334	0.09915	-0.24194	136	0.54049	0.01764	0.11441
37	0.18149	0.61289	-0.30050	87	0.39695	0.09261	-0.23514	137	0.54351	0.02013	0.12189
38	0.18643	0.60124	-0.30604	88	0.40052	0.08632	-0.22825	138	0.54656	0.02282	0.12940
39	0.19136	0.58950	-0.31134	89	0.40406	0.08027	-0.22125	139	0.54965	0.02571	0.13693
40	0.19628	0.57768	-0.31638	90	0.40757	0.07446	-0.21417	140	0.55277	0.02880	0.14448
41	0.20118	0.56579	-0.32116	91	0.41104	0.06890	-0.20700	141	0.55593	0.03210	0.15204
42	0.20608	0.55382	-0.32568	92	0.41448	0.06359	-0.19976	142	0.55912	0.03561	0.15960
43	0.21097	0.54178	-0.32992	93	0.41788	0.05852	-0.19246	143	0.56235	0.03934	0.16717
44	0.21576	0.52990	-0.33388	94	0.42125	0.05370	-0.18510	144	0.56561	0.04329	0.17472
45	0.22048	0.51813	-0.33755	95	0.42458	0.04912	-0.17770	145	0.56891	0.04747	0.18225
46	0.22518	0.50633	-0.34094	96	0.42788	0.04477	-0.17026	146	0.57224	0.05188	0.18976
47	0.22985	0.49451	-0.34404	97	0.43114	0.04066	-0.16279	147	0.57561	0.05653	0.19723
48	0.23451	0.48268	-0.34683	98	0.43437	0.03677	-0.15531	148	0.57901	0.06142	0.20466
49	0.23914	0.47083	-0.34932	99	0.43756	0.03310	-0.14782	149	0.58245	0.06656	0.21202
50	0.24376	0.45898	-0.35150	100	0.44072	0.02966	-0.14032	150	0.58592	0.07195	0.21932

Table 18 TC-72 cross section shape coordinates, Part 2

ID	s	x	y	ID	s	x	y
151	0.58943	0.07759	0.22655	201	0.80312	0.59151	0.33077
152	0.59297	0.08348	0.23369	202	0.80805	0.60368	0.32658
153	0.59655	0.08962	0.24073	203	0.81299	0.61582	0.32217
154	0.60016	0.09601	0.24767	204	0.81795	0.62791	0.31753
155	0.60381	0.10267	0.25448	205	0.82292	0.63995	0.31267
156	0.60748	0.10957	0.26116	206	0.82790	0.65195	0.30759
157	0.61119	0.11672	0.26771	207	0.83290	0.66388	0.30229
158	0.61494	0.12411	0.27411	208	0.83791	0.67576	0.29678
159	0.61871	0.13174	0.28035	209	0.84294	0.68757	0.29105
160	0.62252	0.13962	0.28643	210	0.84797	0.69930	0.28513
161	0.62636	0.14775	0.29232	211	0.85301	0.71097	0.27900
162	0.63023	0.15610	0.29802	212	0.85807	0.72255	0.27267
163	0.63413	0.16468	0.30351	213	0.86313	0.73406	0.26614
164	0.63806	0.17348	0.30880	214	0.86820	0.74547	0.25942
165	0.64203	0.18250	0.31388	215	0.87328	0.75679	0.25251
166	0.64602	0.19173	0.31873	216	0.87836	0.76802	0.24541
167	0.65004	0.20117	0.32334	217	0.88345	0.77914	0.23813
168	0.65408	0.21079	0.32773	218	0.88854	0.79016	0.23067
169	0.65816	0.22060	0.33187	219	0.89364	0.80107	0.22303
170	0.66226	0.23059	0.33578	220	0.89874	0.81187	0.21523
171	0.66640	0.24074	0.33945	221	0.90384	0.82255	0.20726
172	0.67056	0.25105	0.34287	222	0.90894	0.83312	0.19912
173	0.67474	0.26152	0.34604	223	0.91405	0.84356	0.19083
174	0.67895	0.27213	0.34895	224	0.91915	0.85387	0.18238
175	0.68319	0.28288	0.35162	225	0.92425	0.86406	0.17378
176	0.68746	0.29375	0.35404	226	0.92935	0.87411	0.16504
177	0.69175	0.30475	0.35621	227	0.93445	0.88404	0.15616
178	0.69606	0.31586	0.35812	228	0.93954	0.89382	0.14715
179	0.70041	0.32708	0.35978	229	0.94463	0.90347	0.13800
180	0.70477	0.33841	0.36119	230	0.94971	0.91297	0.12874
181	0.70916	0.34982	0.36237	231	0.95479	0.92233	0.11935
182	0.71358	0.36132	0.36327	232	0.95985	0.93154	0.10984
183	0.71802	0.37291	0.36392	233	0.96491	0.94061	0.10023
184	0.72249	0.38456	0.36429	234	0.96996	0.94954	0.09052
185	0.72697	0.39629	0.36440	235	0.97500	0.95831	0.08071
186	0.73149	0.40808	0.36424	236	0.98002	0.96691	0.07079
187	0.73602	0.41992	0.36380	237	0.98504	0.97534	0.06076
188	0.74060	0.43186	0.36311	238	0.99004	0.98356	0.05061
189	0.74532	0.44415	0.36214	239	0.99503	0.99158	0.04033
190	0.75005	0.45644	0.36092	240	1.00000	0.99937	0.02993
191	0.75479	0.46874	0.35943				
192	0.75954	0.48104	0.35769				
193	0.76432	0.49334	0.35569				
194	0.76910	0.50565	0.35344				
195	0.77391	0.51795	0.35093				
196	0.77874	0.53025	0.34818				
197	0.78358	0.54254	0.34517				
198	0.78844	0.55482	0.34193				
199	0.79331	0.56707	0.33845				
200	0.79821	0.57931	0.33472				

Table 19 Cylinder cross section shape coordinates

ID	s	x	y	ID	s	x	y
1	0.00000	1.00000	0.00000	52	0.51000	0.00099	-0.03140
2	0.01000	0.99901	0.03140	53	0.52000	0.00394	-0.06267
3	0.02000	0.99606	0.06267	54	0.53000	0.00886	-0.09369
4	0.03000	0.99114	0.09369	55	0.54000	0.01571	-0.12434
5	0.04000	0.98429	0.12434	56	0.55000	0.02447	-0.15451
6	0.05000	0.97553	0.15451	57	0.56000	0.03511	-0.18406
7	0.06000	0.96489	0.18406	58	0.57000	0.04759	-0.21289
8	0.07000	0.95241	0.21289	59	0.58000	0.06185	-0.24088
9	0.08000	0.93815	0.24088	60	0.59000	0.07784	-0.26791
10	0.09000	0.92216	0.26791	61	0.60000	0.09549	-0.29389
11	0.10000	0.90451	0.29389	62	0.61000	0.11474	-0.31871
12	0.11000	0.88526	0.31871	63	0.62000	0.13552	-0.34227
13	0.12000	0.86448	0.34227	64	0.63000	0.15773	-0.36448
14	0.13000	0.84227	0.36448	65	0.64000	0.18129	-0.38526
15	0.14000	0.81871	0.38526	66	0.65000	0.20611	-0.40451
16	0.15000	0.79389	0.40451	67	0.66000	0.23209	-0.42216
17	0.16000	0.76791	0.42216	68	0.67000	0.25912	-0.43815
18	0.17000	0.74088	0.43815	69	0.68000	0.28711	-0.45241
19	0.18000	0.71289	0.45241	70	0.69000	0.31594	-0.46489
20	0.19000	0.68406	0.46489	71	0.70000	0.34549	-0.47553
21	0.20000	0.65451	0.47553	72	0.71000	0.37566	-0.48429
22	0.21000	0.62434	0.48429	73	0.72000	0.40631	-0.49114
23	0.22000	0.59369	0.49114	74	0.73000	0.43733	-0.49606
24	0.23000	0.56267	0.49606	75	0.74000	0.46860	-0.49901
25	0.24000	0.53140	0.49901	76	0.75000	0.50000	-0.50000
26	0.25000	0.50000	0.50000	77	0.76000	0.53140	-0.49901
27	0.26000	0.46860	0.49901	78	0.77000	0.56267	-0.49606
28	0.27000	0.43733	0.49606	79	0.78000	0.59369	-0.49114
29	0.28000	0.40631	0.49114	80	0.79000	0.62434	-0.48429
30	0.29000	0.37566	0.48429	81	0.80000	0.65451	-0.47553
31	0.30000	0.34549	0.47553	82	0.81000	0.68406	-0.46489
32	0.31000	0.31594	0.46489	83	0.82000	0.71289	-0.45241
33	0.32000	0.28711	0.45241	84	0.83000	0.74088	-0.43815
34	0.33000	0.25912	0.43815	85	0.84000	0.76791	-0.42216
35	0.34000	0.23209	0.42216	86	0.85000	0.79389	-0.40451
36	0.35000	0.20611	0.40451	87	0.86000	0.81871	-0.38526
37	0.36000	0.18129	0.38526	88	0.87000	0.84227	-0.36448
38	0.37000	0.15773	0.36448	89	0.88000	0.86448	-0.34227
39	0.38000	0.13552	0.34227	90	0.89000	0.88526	-0.31871
40	0.39000	0.11474	0.31871	91	0.90000	0.90451	-0.29389
41	0.40000	0.09549	0.29389	92	0.91000	0.92216	-0.26791
42	0.41000	0.07784	0.26791	93	0.92000	0.93815	-0.24088
43	0.42000	0.06185	0.24088	94	0.93000	0.95241	-0.21289
44	0.43000	0.04759	0.21289	95	0.94000	0.96489	-0.18406
45	0.44000	0.03511	0.18406	96	0.95000	0.97553	-0.15451
46	0.45000	0.02447	0.15451	97	0.96000	0.98429	-0.12434
47	0.46000	0.01571	0.12434	98	0.97000	0.99114	-0.09369
48	0.47000	0.00886	0.09369	99	0.98000	0.99606	-0.06267
49	0.48000	0.00394	0.06267	100	0.99000	0.99901	-0.03140
50	0.49000	0.00099	0.03140	101	1.00000	1.00000	0.00000
51	0.50000	0.00000	0.00000				

Table 20 Wind speed and frequency

Wind Speed <i>m/s</i>	Cumulative Distribution
4.0	0.09703
5.0	0.10542
6.0	0.10657
7.0	0.10153
8.0	0.09185
9.0	0.06073
9.5	0.03623
10.0	0.03275
10.5	0.02930
11.0	0.02596
11.5	0.02276
12.0	0.02861
13.0	0.02906
14.0	0.02055
15.0	0.01401
16.0	0.01249
18.0	0.00739
20.0	0.00318
25.0	0.00033

Table 21 Absolute thickness constraint

<i>S</i>	Absolute Thickness [<i>m</i>]
0.00000	5.38000
0.03057	5.36300
0.06222	5.12887
0.09487	4.69181
0.12841	4.16284
0.16274	3.58395
0.19772	3.05710
0.23321	2.66154
0.26907	2.37277
0.30515	2.14436
0.34128	1.95137
0.37731	1.78626
0.41309	1.64011
0.44846	1.49563
0.48328	1.35340
0.51741	1.21399
0.55073	1.07789
0.58312	0.94557
0.61449	0.81742
0.64476	0.69379
0.67385	0.57494
0.70172	0.46110
0.72833	0.35242
0.75364	0.24901
0.77766	0.15091
0.80038	0.05811

Acknowledgments

We acknowledge Birger Luhmann and Niklas Jores from the University of Stuttgart who contributed some results on the tool survey at the beginning of the project.

We further acknowledge the support of Carlo Bottasso from the Technical University of Munich, Rick Damiani from the National Renewable Energy Laboratory in the United States of America and Matthew Lackner from the University of Massachusetts Amherst.

References

- [1] Dykes, K., and Meadows, R., “Applications of Systems Engineering to the Research, Design, and Development of Wind Energy Systems,” Tech. rep., National Renewable Energy Laboratories, 1617 Cole Boulevard, Golden Colorado, USA, December 2011. NREL/TP-5000-52616.
- [2] Bottasso, C., Campagnolo, F., and Croce, A., “Multi-disciplinary constrained optimization of wind turbines,” *Multibody System Dynamics*, Vol. 27, No. 1, 2012, pp. 21–53. URL <http://dx.doi.org/10.1007/s11044-011-9271-x>.
- [3] McWilliam, M. K., “Towards Multidisciplinary Design Optimization Capability of Horizontal Axis Wind Turbines,” Ph.D. thesis, University of Victoria, 2015.
- [4] Zahle, F., Tibaldi, C., Pavese, C., McWilliam, M., Blasques, J. P. A. A., and Hansen, M. H., “Design of an aeroelastically tailored 10 MW wind turbine rotor,” *Journal of Physics: Conference Series*, Vol. 753, 2016. <https://doi.org/10.1088/1742-6596/753/6/062008>.
- [5] Ashuri, T., Martins, J. R. R. A., Zaaijer, M. B., van Kuik, G. A. M., and van Bussel, G. J. W., “Aeroservoelastic design definition of a 20 MW common research wind turbine model,” *Wind Energy*, 2016.
- [6] Scott, S., Capuzzi, M., Langston, D., Bossanyi, E., McCann, G., Weaver, P. M., and Pirrera, A., “Effects of aeroelastic tailoring on performance characteristics of wind turbine systems,” *Renewable Energy*, Vol. 114, 2017, pp. 887 – 903. <https://doi.org/https://doi.org/10.1016/j.renene.2017.06.048>, URL <http://www.sciencedirect.com/science/article/pii/S0960148117305530>.
- [7] Ning, A., Damiani, R., and Moriarty, P., “Objectives and Constraints for Wind Turbine Optimization,” *Journal of Solar Energy Engineering*, Vol. 136, No. 4, 2014, p. 12 pages. <https://doi.org/10.1115/1.4027693>, URL <http://dx.doi.org/10.1115/1.4027693>.
- [8] Gaertner, E., and Lackner, M. A., “Aero-elastic design optimization of floating offshore wind turbine blades,” *2018 Wind Energy Symposium*, 2018.
- [9] Macquart, T., Maes, V., Langston, D., Pirrera, A., and Weaver, P. M., “A New Optimisation Framework for Investigating Wind Turbine Blade Designs,” *Advances in Structural and Multidisciplinary Optimization*, edited by A. Schumacher, T. Vietor, S. Fiebig, K.-U. Bletzinger, and K. Maute, Springer International Publishing, Cham, 2018, pp. 2044–2060.
- [10] Merz, K. O., “Conceptual Design of a Stall-Regulated Rotor for a Deepwater Offshore Wind Turbine,” Ph.D. thesis, NTNU, Department of Civil and Transport Engineering, Trondheim, Norway, 2011.
- [11] Bak, C., Zahle, F., Bitsche, R., Kim, T., Yde, A., Henriksen, L. C., Natarajan, A., and Hansen, M. H., “Description of the DTU 10 MW Reference Wind Turbine,” Tech. rep., Technical University of Denmark Institute for Wind Energy, 2013.
- [12] Wächter, A., and Biegler, L. T., “On the implementation of an interior-point filter line-search algorithm for large-scale nonlinear programming,” *Mathematical Programming*, Vol. 106, No. 1, 2006, pp. 25–57. <https://doi.org/10.1007/s10107-004-0559-y>, URL <https://doi.org/10.1007/s10107-004-0559-y>.
- [13] Deb, K., Pratap, A., Agarwal, S., and Meyarivan, T., “A fast and elitist multiobjective genetic algorithm: NSGA-II,” *IEEE Transactions on Evolutionary Computation*, Vol. 6, No. 2, 2002, pp. 182–197. <https://doi.org/10.1109/4235.996017>.
- [14] Manwell, J. F., McGowan, J. G., and Rogers, A. L., *Wind Energy Explained, Theory, Design and Application*, John Wiley and Sons, Chichester, England, 2002.